

國立交通大學  
材料科學與工程學系  
博士論文

鐵鋁錳碳合金之相變化及機械性質



研究生：王承舜  
指導教授：劉增豐 博士  
                  朝春光 博士

中華民國九十六年七月

# Phase Transitions and Mechanical Properties of the Fe-Al-Mn-C Alloys

研究生：王承舜

Student: Cheng-Shun Wang

指導教授：劉增豐 博士

Advisor: Dr. Tzeng-Feng Liu

朝春光 博士

Dr. Chuen-Guang Chao

國立交通大學

材料科學與工程學系

博士論文



Submitted to Department of Materials Science and Engineering  
College of Engineering

National Chiao Tung University

in Partial Fulfillment of the Requirements

for the Degree of

Doctor of Philosophy

in

Materials Science and Engineering

July 2007

Hsinchu, Taiwan, Republic of China

中華民國九十六年七月

## 誌 謝

感謝主的恩典，在我身上一再印證祂能給我們的恩賜有多豐盛。

另外最需要由衷感謝的就是指導教授劉增豐博士與朝春光教授數年來悉心指導與諄諄教誨，使學生能順利完成此論文。不管在學術上的成就或是為人處事的態度方面，兩位老師的身教與言教絕對能讓學生一生受用不盡，而在最後階段兩位老師更為了學生犧牲自己陪伴家人的時間，更是讓學生不曉得如何表達心中的感激，只能說我非常的幸運，才能碰到兩位這麼關心學生的好老師。在生活上，特別感謝吾師劉增豐教授與師母林美慧老師時時的關懷和鼓勵，謹致最高的敬意與誠摯的謝忱。口試時承蒙賀俊教授、莊振益教授、黃俊銘博士等口試委員悉心指正，更令學生受益匪淺。

感謝我的父母與家人在這段時間對我的支持與鼓勵，雖然最疼愛我的先祖父文季公來不及聽到我親口告訴他論文完成的好消息，但我相信他在主的懷抱裡一定已經知道了這個消息而且會非常欣慰。

感謝交大棒球隊的黃杉楹教練以及球隊的全體成員，跟大家一起奮鬥了這麼多年，我必須要說：跟你們並肩作戰的感覺真好。

感謝實驗室的學長學弟們對我的幫助，學長李堅瑋博士、鄭祥誠博士、譚澤安博士、吳忠春博士以及黃志能博士對我毫不藏私的幫助跟指教，另外同學跟學弟們也一直對我提供非常多的幫助，包括陳志壕博士、楊勝裕博士、跟最近盡心幫助我的逸軒、俊瑋、志龍、世陽、信良、浩仰、雨霖、柏至、哲郎、敬恆、欣龍...以及其他說之不盡曾經在鐵鋁錳實驗室共事過的同學與學弟們，我會非常懷念這段我們一起同甘苦的日子。祝福已經畢業的各位都有好的發展，還在努力中的各位也都能早日順利完成學業。此外，國科會在研究經費上之贊助，使得本論文得以順利完成，在此一併致上衷心的謝意。

最後，僅將論文獻給我最愛的父母親、家人及美琴，感謝他們多年來的辛勞、支持與鼓勵，使我能無後顧之憂地完成學業。同時也感謝所有關心我的親友們。

2007/7/27 於交大工六館 501 室

# 鐵鋁錳合金之相變化及機械性質

研究生：王承舜

指導教授：劉增豐 博士

朝春光 博士

國立交通大學材料科學與工程研究所

## 中文摘要

本論文研究 Fe-9Al-30Mn-2.0C 合金之相變化及 Fe-9Al-30Mn-1.0C 與 Fe-9Al-30Mn-2.0C 合金之顯微結構與機械性質。依據實驗的結果，本論文所得到的具體研究結果如下：



(一)、在淬火狀態下，Fe-9wt.%Al-30wt.%Mn-2.0wt.%C合金的顯微結構為沃斯田鐵相中包含細微的 $(\text{Fe,Mn})_3\text{AlC}$ 碳化物（K'碳化物）。其中具備 $L'1_2$ 結構的細微K'碳化物是在淬火過程中藉由史賓諾多相分解反應產生，當此合金在 550 至 900°C時效處理後，細微的K'碳化物會在沃斯田鐵相基地內成長，而粗大的 $(\text{Fe,Mn})_3\text{AlC}$ 碳化物（K碳化物）開始在晶界上出現。當此合金在 900 至 1100°C時效處理後，粗大的K碳化物及細微的K'碳化物會同時在沃斯田鐵相基地內出現，這個結果以前未曾被其他學者在鐵鋁錳系合金中觀察到過。另外，在晶界上析出的粗大K碳化物中，鋁及錳的含量會隨著時效溫度而變化。

(二)、我們研究了以傳統鑄造方式製備的 Fe-9wt.%Al-30wt.%Mn-2.0wt.%C 合金的機械性質，由拉伸測試的結果我們發現在淬火狀態下此合金具有最佳的抗拉強度及延性組合，此時此合金具有很好的最大抗拉強度 (UTS) 1060 MPa 及極佳的 57%伸長率。當此合金在 750°C 時效處理後，我們發現合金的強度及延性都隨著時間增加而明顯下降，此合金在淬火狀態下的強度及延性都要比時效處理過的合金優異許多。值得注意的是以往未曾有學者研究過高碳含量(大於 1.3%)的沃斯田鐵系鐵鋁錳合金的機械性質。另外我們也發現此合金在時效處理後所形成的  $\gamma/\kappa$  層狀結構並不會改善合金的延性，這是因為細微的裂縫會在  $\kappa$  碳化物中起始並連結造成劈裂。

(三)、在淬火狀態下 Fe-9wt.%Al-30wt.%Mn-1.0wt.%C 合金的顯微結構為單一沃斯田鐵相，在 625°C 短時間時效處理後，細微的  $\kappa'$  碳化物會出現在沃斯田鐵相基地內；在 625°C 延長時效時間做時效處理後，細微的  $\kappa'$  碳化物會在基地內成長，且可以在晶界上觀察到  $\gamma + \kappa'$  碳化物  $\rightarrow \gamma +$  粗大  $\kappa$  碳化物的反應，此 ( $\gamma + \kappa$ ) 的混合相具有層狀的結構。由拉伸測試的結果知道雖然此合金在經過 96 小時的長時間時效後會有 ( $\gamma + \kappa$ ) 的層狀結構出現在晶界上，此合金仍然具有很好的 28%伸長率。這是因為 ( $\gamma + \kappa$ ) 的層狀結構所佔的比率很小，尚不至於對延性影響太大。

# Phase Transitions and Mechanical Properties of the Fe-Al-Mn-C Alloys

Student: Cheng-Shun Wang      Advisor: Dr. Tzeng-Feng Liu

Dr. Chuen-Guang Chao

Department of Materials Science and Engineering

National Chao Tung University



## Abstract

Phase transitions in an Fe-9Al-30Mn-2.0C alloy, and the mechanical properties of the Fe-9Al-30Mn-1.0C and Fe-9Al-30Mn-2.0C alloys have been investigated. On the basis of the experimental examinations, some results can be summarized as follows:

[1]. The as-quenched microstructure of the Fe-9wt.%Al-30wt.%Mn-2.0wt.%C alloy was austenite phase containing fine  $(\text{Fe,Mn})_3\text{AlC}$  carbides. The fine  $(\text{Fe,Mn})_3\text{AlC}$  carbides having an  $L'1_2$  structure were formed by spinodal decomposition during quenching. When the as-quenched alloy was aged at 550-900°C for moderate times, the fine  $(\text{Fe,Mn})_3\text{AlC}$  carbides grew within the austenite matrix and coarse  $(\text{Fe,Mn})_3\text{AlC}$  carbides started to

occur on the austenite grain boundaries. When the alloy was aged at 900-1100°C and then quenched, both of large and extremely fine (Fe,Mn)<sub>3</sub>AlC carbides could be observed simultaneously within the austenite matrix. This feature has never been observed by other workers in the Fe-Al-Mn-C alloy systems before. Furthermore, the Al and Mn concentrations in the coarse (Fe,Mn)<sub>3</sub>AlC carbides formed on the grain boundaries were found to vary drastically with the aging temperature.

[2]. The mechanical properties of the Fe-9wt.%Al-30wt.%Mn-2.0wt.%C alloy, prepared by conventional casting process, were examined. Tensile tests revealed that the optimal combination of mechanical strength and ductility of the alloy was the as-quenched specimen which had good ultimate tensile strength (UTS) of 1060 MPa with an excellent 57% elongation. When the as-quenched alloy was aged at 750 °C for 3-96 h, both the tensile strength and ductility were significantly decreased. Interestingly, both of the mechanical strength and ductility of the as-quenched specimen were much better than those of the aged specimens. It is worthwhile to note that the mechanical properties of the austenitic Fe-Al-Mn-C alloys with C > 1.3 wt.% in the as-quenched condition have never been investigated by other workers before. In addition, the  $\gamma/\kappa$  lamellar structure of the aged specimens could not improve the tensile ductility because sub-cracks initiated at coarsened  $\kappa$  carbides and linked up to trigger cleavage.

[3]. The as-quenched microstructure of the Fe-9wt.%Al-30wt.%Mn-1.0wt.%C

alloy was a single austenite ( $\gamma$ ) phase. When the alloy was aged at  $625^{\circ}\text{C}$  for short times, fine  $(\text{Fe,Mn})_3\text{AlC}$  carbides ( $\kappa'$  carbides) were observed to precipitate within the  $\gamma$  matrix. After prolonged aging at  $625^{\circ}\text{C}$ , the fine  $(\text{Fe,Mn})_3\text{AlC}$  carbides grew within the  $\gamma$  matrix and a  $\gamma + \kappa' \rightarrow \gamma + \text{coarse } (\text{Fe,Mn})_3\text{AlC carbide } (\kappa \text{ carbide})$  reaction occurred on the grain boundaries. The mixture of ( $\gamma + \kappa$  carbides) had a lamellar structure. Tensile tests revealed that although the  $\gamma/\kappa$  lamellar structure occurred on the  $\gamma/\gamma$  grain boundaries after aged at  $625^{\circ}\text{C}$  for 96 h, the present alloy still exhibited good 28% elongation. Because the area fraction of the  $\gamma/\kappa$  lamellar structure exhibited in the aged alloy was still very small, its influence on the ductility wasn't pronounced.





# Contents

	<u>page</u>
中文摘要 .....	i
Abstract .....	iii
Contents .....	vi
List of Tables .....	viii
List of Figures .....	ix
<b>Chapter 1. General Introduction .....</b>	<b>1</b>
1-1 The Development of Fe-Al-Mn-C Alloys as the Substitutes for High Strength-High Ductility Steels .....	2
1-2 The Purposes of This Study .....	10
References .....	12
<b>Chapter 2. Phase Transitions in an Fe-9Al-30Mn-2.0C Alloy .....</b>	<b>17</b>
2-1 Introduction .....	19
2-2 Experimental Procedure .....	21
2-3 Results and Discussion .....	23
2-4 Conclusions .....	29
References .....	30

<b>Chapter 3. Mechanical Properties of an Fe-9Al-30Mn-2.0C Alloy</b>	<b>42</b>
3-1 Introduction	45
3-2 Experimental Procedure	49
3-3 Results and Discussion	51
3-4 Conclusions	55
References	56
<b>Chapter 4. Mechanical Properties of an Fe-9Al-30Mn-1.0C Alloy</b>	<b>64</b>
4-1 Introduction	67
4-2 Experimental Procedure	71
4-3 Results and Discussion	73
4-4 Conclusions	78
References	80
<b>Chapter 5. Summary</b>	<b>92</b>
<b>List of Publications</b>	<b>95</b>

## List of Tables

Table 2.1 Chemical compositions of the  $\kappa$  carbide revealed by EDS.....41

Table 4.1 Area fractions of the  $\gamma/\kappa$  lamellar structure.....91



## List of Figures

Figure 1.1	(a) L'12 crystal structure. (b) L12 crystal structure.....	16
Figure 2.1	Transmission electron micrographs of the as-quenched alloy: (a) BF, (b) an SADP taken from the mixed region of austenite matrix and fine $\kappa'$ carbides. The foil normal is [001] (hkl: austenite matrix; hkl: $\kappa'$ carbide), and (c) DF obtained by use of the (100) $\kappa'$ superlattice reflection in the [001] zone.....	31
Figure 2.2	Transmission electron micrographs of the alloy aged at 550°C for 12 h: (a) BF, and (b) an SADP taken from the $\kappa$ carbide marked as “K” in (a).....	33
Figure 2.3	BF electron micrographs of the alloy aged at 550°C for (a) 32 h, and (b) 48 h.....	34
Figure 2.4	Transmission electron micrographs of the alloy aged at 900°C for 4 h. (a) BF, (b) an SADP taken from the region marked as “A” in (a), (c) BF, (d) (100) $\kappa'$ DF, and (e) an SADP taken from the coarse $\kappa$ carbide marked as “K” in (c).....	35
Figure 2.5	BF electron micrograph of the alloy aged at 1150°C for 1 h .....	38
Figure 2.6	Three typical EDS spectra taken from the coarse $\kappa$ carbide in	

	the alloy aged at (a) 550°C, (b) 750°C, and 900°C, respectively.....	39
Figure 3.1	Micrographs of the Fe-9%Al-30%Mn-2.0% C alloy in the as-quenched condition. (a) an optical micrograph, (b) a selected-area diffraction pattern taken from the mixed region of austenite matrix and fine $\kappa'$ carbides. The foil normal is [001] (hkl: austenite matrix; hkl: $\kappa'$ carbide), and (c) a dark-field (DF) electron micrograph taken by (100) $\kappa'$ superlattice reflection in [001] zone.....	58
Figure 3.2	SEM micrographs of the alloy aged at 750°C for (a) 24 h, and (b) 96 h.....	60
Figure 3.3	Tensile test results of the alloy in the as-quenched condition and after aged at 750°C for various times.....	61
Figure 3.4	SEM micrographs of the fractured specimen. (a) and (b), fracture and free surfaces of the as-quenched specimen, respectively. (c) and (d), fracture and free surfaces of the specimen aged at 750°C for 24 h, respectively.....	62
Figure 4.1	An optical micrograph of the as-quenched Fe-9%Al-30%Mn-1.0% C alloy.....	82
Figure 4.2	Transmission electron micrographs of the alloy aged at 625°C	

for 6 h. (a) bright-field, (b) a selected-area diffraction pattern taken from a mixed region of austenite matrix and fine  $\kappa'$  carbides. The foil normal is  $[001]$  ( $hkl$ : austenite matrix;  $hkl$ :  $\kappa'$  carbide), and (c) a dark-field (DF) electron micrograph taken by  $(100)\kappa'$  superlattice reflection in the  $[001]$  zone.....83

Figure 4.3 Bright-field electron micrograph of the alloy aged at  $625^{\circ}\text{C}$  for 24 h .....85

Figure 4.4 Micrographs of the alloy aged at  $625^{\circ}\text{C}$  for 96 h. (a) a SEM micrograph, (b)-(c) TEM micrographs: (b) bright-field, and (c) a selected-area diffraction pattern taken from the  $\kappa$  carbide marked as “K” in (b) and its surrounding austenite phase. The foil normal is  $[001]$  ( $hkl$ : austenite phase;  $hkl$ :  $\kappa$  carbide).....86

Figure 4.5 Tensile test results of the alloy in the as-quenched condition and after aged at  $625^{\circ}\text{C}$  for various times.....88

Figure 4.6 SEM micrographs of the fractured specimen aged at  $625^{\circ}\text{C}$  for 24 h. (a) fracture surface and (b) free surface contiguous to the fracture surface.....89

Figure 4.7 SEM micrographs of the fractured specimen aged at  $625^{\circ}\text{C}$  for 96 h. (a) fracture surface and (b) free surface contiguous to the fracture surface.....90

# Chapter 1.

## General Introduction



## **1-1 The Development of Fe-Al-Mn-C Alloys as the Substitutes for High Strength-High Ductility Steels**

In the past years, a considerable amount of interest has been expressed in the possibility of developing Fe-Al-Mn-C alloys as high strength-high ductility alloy steels [1-25]. In the Fe-Al-Mn-C alloy systems, manganese and carbon can enhance the stability of the austenitic structure which has a better workability and low-temperature ductility. Aluminum is a ferrite stabilizer and plays an important role in the high-temperature oxidation resistance. An increase in the aluminum content will be beneficial to the mechanical strength of the alloy. The amount of manganese required to produce a f.c.c. structure depends on the contents of aluminum and carbon in the alloy. In general, the f.c.c. structure can be stabilized by increasing the contents of manganese and carbon, or decreasing the content of aluminum. It is well-known that through a proper combination of aluminum, manganese and carbon, an alloy with a fully austenitic structure can be achieved. In the Fe-Al-Mn-C alloy systems, it is known that after being solution heat treated and aged at temperatures ranging from 450 to 650°C for moderate times, the austenitic alloy can possess a remarkable combination of strength and ductility, which is attributed to the formation of extremely fine  $(\text{Fe,Mn})_3\text{AlC}$  carbides within the austenite matrix [11-20].



In the Fe-Al-Mn-C alloys with lower carbon contents, the microstructure containing duplex (ferrite + austenite) phases could be observed in the as-quenched condition [14,24-26], and  $(\text{Fe,Mn})_3\text{AlC}$  carbides,  $\beta\text{-Mn}$  precipitates as well as  $\text{D0}_3$  phases were examined in the aged specimens. Besides the duplex (ferrite + austenite) Fe-Al-Mn-C alloys, the phase transitions in the austenitic Fe-Al-Mn-C alloys prepared by conventionally casting process have also been studied by many workers [11-18]. In their studies, it is found that when an alloy with a chemical composition in the range of Fe-(4.9-11)Al-(28-35)Mn-(0.5-1.3)C was solution heat-treated and then quenched rapidly, the microstructure was single-phase austenite. After being aged at temperatures ranging from 500 to 750°C for moderate times [11,14-24], fine and coarse  $(\text{Fe,Mn})_3\text{AlC}$  carbides started to precipitate coherently within the austenite matrix and heterogeneously on the austenite grain boundaries in a form of coarse particle, respectively. Both of the fine and coarse  $(\text{Fe,Mn})_3\text{AlC}$  carbides have an  $\text{L}'1_2$  structure [22,27-31]. For convenience, the  $\kappa'$  carbide and  $\kappa$  carbide were used to represent the  $(\text{Fe,Mn})_3\text{AlC}$  carbide formed within the austenite matrix and heterogeneously on the austenite grain boundaries, respectively. After prolonged aging, the coarse  $\kappa$  carbides grew into the adjacent austenite grains through a  $\gamma \rightarrow \gamma_0$  (carbon-lack austenite) +  $\kappa$  carbide reaction, a  $\gamma \rightarrow \alpha$  (ferrite) +  $\kappa$  carbide reaction, a  $\gamma \rightarrow \kappa$  carbide +  $\beta\text{-Mn}$  reaction,

a  $\gamma \rightarrow \alpha + \kappa$  carbide +  $\beta$ -Mn reaction, or a  $\gamma \rightarrow \alpha + \beta$ -Mn reaction [29-34], depending on the chemical composition and aging temperature. In addition, it was reported that the precipitation on the  $\gamma/\gamma$  grain boundaries, such as coarse  $\kappa$  carbides, ferrite phases and  $\beta$ -Mn precipitates, resulted in the embrittlement of the alloy [31,32].

Besides the conventionally casting process prepared Fe-Al-Mn-C alloys, phase transformations in the Fe-(2-10)Al-(20-31.9)Mn-(0.74-4.3)C alloys, prepared by rapid solidification (RSP), have been studied chiefly by J. A. Sarreal, C. C. Koch, K. H. Han and W. K. Choo [21,35-38]. Based on their studies, it is found that in the as-RS condition, the microstructure of the Fe-8.8Al-31.5Mn-xC alloy with  $0.74 \leq x \leq 1.62$  wt.% was single-phase austenite  $\gamma$ . When the carbon content was increased to 2.02 wt.% or above, fine  $\kappa'$  carbides having an L'1<sub>2</sub>-type structure could be formed within the austenite matrix during the rapid solidification process. This means that the carbon content may play an important role in the formation of fine  $\kappa'$  carbides in the as-RS Fe-Al-Mn-C alloys. When the alloys were aged at temperature ranging from 550 to 650°C for moderate times, the (Fe,Mn)<sub>3</sub>AlC carbides were found to occur not only within the austenite matrix, but also heterogeneously on the austenite grain boundaries in a form of coarse particle. With increasing the aging time within this temperature range, the coarse  $\kappa$  carbides grew into the

adjacent austenite grains through a  $\gamma \rightarrow \alpha + \kappa$  transition in the alloys containing higher carbon (i.e., 1.62 wt.%) and a  $\gamma \rightarrow \alpha + \kappa + \beta$ -Mn transition in the alloys containing lower carbon contents (i.e., 0.98 wt.%) [18,36-46]. Obviously, the phase transformation behaviors in the Fe-Al-Mn-C alloys with lower carbon content, prepared by RSP, are similar to those examined in the conventionally prepared ones.

Besides the extensive studies of the Fe-Al-Mn-C alloys with  $C \leq 1.3$  wt.%, the phase transitions in the conventionally prepared Fe-Al-Mn-C alloys with higher carbon content have also been examined by several workers [47-49]. Based on their studies, it is obvious that the as-quenched microstructure of the Fe-(6-9)Al-(26-30.7)Mn-(1.5-2.8)C alloys was austenite phase containing fine  $\kappa'$  carbides [47,48]. This is quite different from that observed in the austenitic Fe-Al-Mn-C alloys with  $C \leq 1.3$  wt.% . It seems to imply that the carbon content may play an important role in the formation of fine  $\kappa'$  carbides within the austenite matrix during quenching. When the Fe-Al-Mn-C alloys with  $1.5 \leq C \leq 2.8$  wt.% were aged between 800-1200°C for longer times, the stable microstructure was found to be the mixture of (austenite phase +  $\kappa$  carbide) [47-49]. Moreover, it is worthwhile to discuss the structure of the  $\kappa$  ( $\kappa'$ ) carbide formed in the Fe-Al-Mn-C alloys. In the previous studies, it was always reported that the  $\kappa$  carbides has an  $L1_2$  type structure [38-41]. However, Sarreal and

Koach suggested that the  $\kappa$  carbides has an  $L1_2$  and  $L'1_2$  structure [38]. The only difference between the  $L1_2$  and  $L'1_2$  structure is the degree of order of the carbon atom arrangement. The carbon atoms are randomly situated on octahedral site for the  $L1_2$  structure, while they are all located in the body-centered, octahedral site for the  $L'1_2$  structure, as shown in Figure 1.1. In the previous studies, it is clearly seen that most examinations of the Fe-Al-Mn-C alloys with higher carbon were only focused on the alloys at 800°C or above. Little information was available concerning the microstructural developments of the alloys at lower temperature. Therefore, one of the purposes of this work is an attempt to study the phase transitions in the Fe-9Al-30Mn-2.0C alloy heat-treated at 550-1200°C.

In previous studies concerning the mechanical properties of the Fe-Al-Mn-C alloys, it was reported that the grain boundary precipitates resulted in the embrittlement of the austenitic Fe-Al-Mn-C alloys [31,32,41]. For example, in the previous studies in the Fe-7.8Al-30Mn-1.3C alloy [31], it was reported that the as-quenched alloy exhibited yield strength (YS) 475 MPa with 57% elongation. Optimal mechanical properties (YS 1080 MPa and ultimate tensile strength (UTS) 1120 MPa) could be attained when the alloy was aged at 550°C for about 100 h; however, when the alloy was further aged at 550°C, both YS and UTS decreased with prolonged aging time and the alloy finally

became extremely brittle.

Besides the extensive studies of the Fe-Al-Mn-C alloys with  $C \leq 1.3$  wt.%, the microstructures in the conventionally prepared Fe-Al-Mn-C alloys with higher carbon content have also been examined by several workers [47-49,51]. Based on their studies, it is obvious that the as-quenched microstructure of the Fe-(6-9)Al-(26-30.7)Mn-(1.5-2.8)C alloys was austenite phase containing fine  $\kappa'$  carbides [47,48,51]. This is quite different from that observed in the austenitic Fe-Al-Mn-C alloys with  $C \leq 1.3$  wt.%. When the Fe-Al-Mn-C alloys with  $1.5 \leq C \leq 2.8$  wt.% were aged between 800 and 1200°C for longer times, the stable microstructure was found to be a lamellar product of  $\gamma + \kappa$  [47-49]. Although the microstructures have been extensively studied, information concerning the mechanical properties in the conventionally prepared Fe-Al-Mn-C alloys with higher C contents is very deficient. We are aware of only one article [48]. It was reported that in the furnace-cooled condition, the Fe-15at.%Al-26at.%Mn-8at.%C (Fe-8.5Al-29.5Mn-2.0C, in wt.%) alloy exhibited almost zero ductility. In order to improve the ductility, the alloy was solution heat-treated at 1100°C for 1 h followed by water quenched, and subsequently aged at 800°C for 120 h. It was observed that the  $\gamma/\kappa$  lamellar structure was formed in the alloy after the heat treatment. By forming the  $\gamma/\kappa$  lamellar structure, the elongation could be drastically improved to be about 10% with YS 675 MPa and UTS 1020 MPa.

Besides this, little information was available concerning the mechanical properties of the Fe-Al-Mn-C alloys with higher C ( $C > 1.3$  wt.%) content. Therefore, one of the purposes of this work is an attempt to study the mechanical properties in the Fe-9Al-30Mn-2.0C alloy.

In our study concerning the mechanical properties of the Fe-9Al-30Mn-2.0C, several interesting results were obtained. After prolonged aged at  $750^{\circ}\text{C}$ , the final microstructure of the Fe-9Al-30Mn-2.0C alloy was  $\gamma/\kappa$  lamellar structure. Tensile tests revealed that the optimal combination of mechanical strength with ductility of the alloy was the as-quenched specimen which had good ultimate tensile strength (UTS) of 1060 MPa with an excellent 57% elongation. The UTS values of all the aged specimens decreased and the tensile ductility drastically dropped. Obviously, the mechanical property of the as-quenched specimen is much better than that of aged ones. The result has never been reported in previous literatures for the austenitic Fe-Al-Mn-C alloys with higher C content ( $C \geq 1.3$  wt.%) prepared by conventional casting process. In addition, the  $\gamma/\kappa$  lamellar structure of aged specimens could not improve tensile ductility because crack initiated at coarsened  $\kappa$  carbides and linked up. However, in the previous studies, little information concerning the  $\gamma/\kappa$  lamellar structural influence on the mechanical properties was provided. In order to clarify this feature, the purpose of this study is an attempt to study the

mechanical properties in the Fe-9Al-30Mn-1.0C alloy.



## **1-2 The Purposes of This Study**

The purposes of this study are summarized as follows:

- (1) Concerning the phase transitions in the Fe-9Al-30Mn-2.0C alloy heat-treated at 550-1200°C, it is seen that most examinations of the Fe-Al-Mn-C alloys with higher carbon were only focused on the alloys at 800°C or above. Little information was available concerning the microstructural developments of the alloys at lower temperature. Therefore, the purpose of this work is an attempt to study the phase transitions in the Fe-9Al-30Mn-2.0C alloy heat-treated at 550-1200°C by using optical microscopy and transmission electron microscopy.
- (2) Examining the mechanical properties in the conventionally prepared Fe-Al-Mn-C alloys with higher C contents. It was reported that in the furnace-cooled condition, the Fe-15at.%Al-26at.%Mn-8at.%C (Fe-8.5Al-29.5Mn-2.0C, in wt.%) alloy exhibited almost zero ductility. In order to improve the ductility, the alloy was solution heat-treated at 1100°C for 1 h followed by water quenched, and subsequently aged at 800°C for 120 h. It was observed that the  $\gamma/\kappa$  lamellar structure was formed in the alloy after the heat treatment. By forming the  $\gamma/\kappa$  lamellar structure, the elongation could be drastically improved to be about 10% with YS 675 MPa and UTS



1020 MPa. Besides this, little information was available concerning the mechanical properties of the Fe-Al-Mn-C alloys with higher carbon content ( $C > 1.3$  wt.%). Therefore, the purpose of this work is an attempt to study the mechanical properties in the Fe-9Al-30Mn-2.0C alloy.

- (3) To investigate the influence of  $\gamma/\kappa$  lamellar structure on the mechanical properties of the Fe-Al-Mn-C alloys with lower carbon contents ( $C < 2.0$  wt.%). In our previous study concerning the mechanical properties in the Fe-9Al-30Mn-2.0C alloy, it is obvious that the mechanical property of the as-quenched specimen is much better than that of aged ones. In addition, the  $\gamma/\kappa$  lamellar structure of aged specimens could not improved tensile ductility because sub-crack initiated at coarsened  $\kappa$  carbides and linked up to trigger cleavage. However, little information concerning the effect of  $\gamma/\kappa$  lamellar structure on the mechanical properties of the Fe-Al-Mn-C alloys with lower carbon contents ( $C < 2.0$  wt.%). Therefore, the purpose of this study is an attempt to study the mechanical properties in the Fe-9Al-30Mn-1.0C alloy.

## References

- [1] T.F. Liu, C.M. Wan, Studies of Microstructures and Strength of Fe-Al-Mn Alloys, Proc. 7th Int. Conf. on the Strength of Metals and Alloys, Montreal, Canada, Aug. (1985) 423.
- [2] S.M. Zhu, S.C. Tjong, *Metalls. Trans. A* 29 (1998) 299.
- [3] I.S. Kalashnikov, O Acselrad, L.C. Pereira, T. Kalichak, M.S. Khadyev, *J Mater. Eng. Perform.* 9 (2000) 334.
- [4] S.C. Chang, Y.H. Hsiau, *J. Mater. Sci.* 24 (1989) 1117.
- [5] S.C. Chang, W.H. Weng, H.C. Chen, S.J. Lin, P.C.K. Chung, *Wear* 181-183 (1995) 511.
- [6] S.C. Tjong, C.S. Wu, *Mater. Sci. Eng.* 80 (1986) 203.
- [7] W.T. Tsai, J.B. Duh, J.T. Lee, *J. Mater. Sci.* 22 (1987) 3517.
- [8] C.J. Wang, Y.C. Chang, *Mater. Chem. Phy.* 2002; 76: 151-161.
- [9] I.F. Tsu, T.P. Perng, *Metall. Trans. A* 22 (1991) 215.
- [10] S.M. Zhu, S.C. Tjong, *Scripta* 36 (1997) 317.
- [11] S.K. Banerji, *Met. Prog.* (1978) 59.
- [12] H.W. Leavenworth, Jr. and J.C. Benz, *J. Met.* (1985) 36.
- [13] J. Charles, A. Berghezan , A. Lutts, P.L. Dancoisne, *Met. Prog.* (1981) 71.
- [14] R. Wang, F.H. Beck, *Met. Prog.* (1983) 72.

- [15] J.C. Garcia, N. Rosas, R.J. Rioja, *Met. Prog.* (1982) 47.
- [16] D.J. Schmatz, *Trans. ASM.* 52 (1960) 898.
- [17] M.F. Alekseyenko, G.S. Krivonogov, L.G. Kozyreva, I.M. Kachanova, L.V. Arapova, *Met. Sci. Heat Treat.* 14 (3-4) (1972) 187.
- [18] L.I. Lysak, M.F. Alekseyenko, A.G. Drachinskaya, N.A. Storchak, G.S. Krivonogov, *Metallofizika.* 59 (4) (1975) 29.
- [19] R.E. Cairns, Jr. and J.L. Ham, U.S. Patent, No. 3111405 (1963).
- [20] I. Briggs, G.J. Russell, A.G. Clegg, *J. Mater. Sci.* 20 (1985) 668.
- [21] W.K. Choo, K.H. Han, *Metall. Trans. A.* 16 (1985) 5.
- [22] K.H. Han, J.C. Yoon, W.K. Choo, *Scripta Metall.* 20 (1986) 33.
- [23] W.K. Choo, D.G. Kim, *Metall. Trans. A.* 18 (1987) 759.
- [24] S.C. Tjong, N.G. Ho, *Metallography.* 21 (1988) 199.
- [25] G.L. Kayak, *Met. Sci. Heat Treat.* 22 (2) (1969) 95.
- [26] C.C. Wu, J.S. Chou, T.F. Liu, *Metall. Trans. A* 22 (1991) 2265.
- [27] K. Sato, K. Tagawa, Y. Inoue, *Scripta Metall.* 22 (1988) 899.
- [28] C.N. Hwang, T.F. Liu, *Scripta Mater.* 36 (1997) 853.
- [29] C.N. Hwang, C.Y. Chao, T.F. Liu, *Scripta Metall.* 28 (1993) 263.
- [30] C.Y. Chao, C.N. Hwang, T.F. Liu, *Scripta Metall.* 28 (1993) 109.
- [31] W.K. Choo, J.H. Kim, J.C. Yoon, *Acta Mater.* 45 (1997) 4877.
- [32] I.S. Kalashnikov, O. Acselrad, A. Shalkevich, *J. Mater. Processing*

Technology 136 (2003) 72.

- [33] G.S. Krivonogov, M.F. Alekseyenko, G.G. Solov'yeva, Fiz. Metal. Metalloved. 39 (1975) 86.
- [34] K. Sato, K. Tagawa, Y. Inoue, Metal. Trans. A 21 (1990) 5.
- [35] K.H. Han, W.K. Choo, Metall. Trans. A 20 (1989) 205.
- [36] K.H. Han, W.K. Choo, Metall. Trans. A 14 (1983) 973.
- [37] K.H. Han, W.K. Choo, D.E. Laughlin, Scripta Metall. 22 (1988) 1873.
- [38] J.A. Sarreal, C.C. Koch, Mater. Sci. Eng. A 136 (1991) 141.
- [39] J.E. Krzanowski, Metall. Trans. A 19 (1988) 1873.
- [40] P.J. James, J. Iron Steel Inst. (1969) 54.
- [41] K. Sato, K. Tagawa, Y. Inoue, Mater. Sci. Eng. A 111 (1989) 45.
- [42] S.C. Tjong, Mater. Char. 24 (1990) 275.
- [43] T.F. Liu, J.S. Chou, C.C. Wu, Metall. Trans. A 21 (1990) 1891.
- [44] C.Y. Cho, T.F. Liu, Scripta Metall. 25 (1991) 1623.
- [45] A. Inoue, Y. Kojima, T. Minemura, T. Masumoto, Trans. Jph. Inst. 20 (1979) 468.
- [46] A. Inoue, T. Minemura, A. Kitamura, T. Masumoto, Metall. Trans. A 12 (1981) 1041.
- [47] K. Ishida, H. Othani, N. Satoh, R. Kainuma, T. Nishizawa, ISIJ International 30 (1990) 680.

- [48] Y. Kimura, K. Handa, K. Hayashi, Y. Mishima, *Intermetallics* 12 (2004) 607.
- [49] Y. Kimura, K. Hayashi, K. Handa, Y. Mishima, *Mater. Sci. Eng. A* 329-331 (2002) 680.
- [50] Y. Ikarashi, K. Sato, T. Yamazaki, Y. Inoue, M. Yamanaka, *J. Mater. Sci. Letters* 11 (1992) 733.
- [51] C.Y. Chao, L. K. Hwang, T. F. Liu: *Scripta Metall.* 29 (1993) 647.



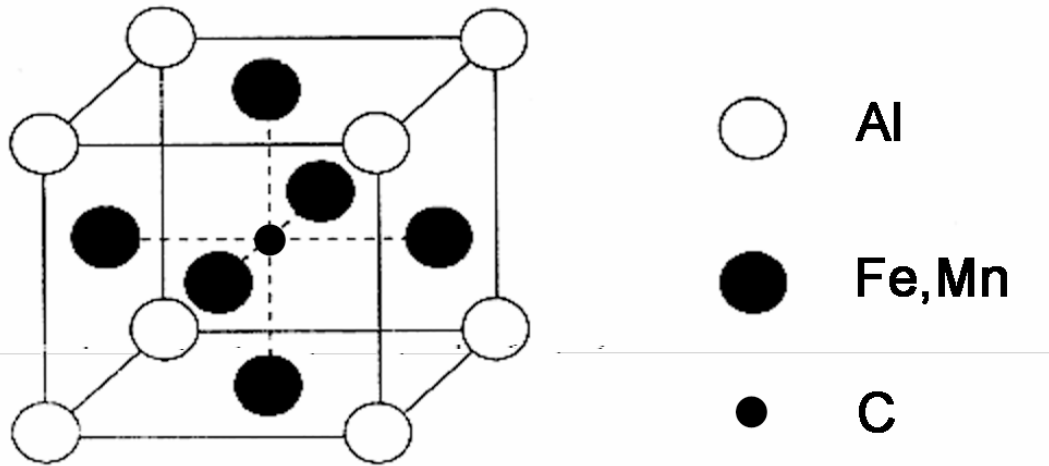


Figure 1.1(a)

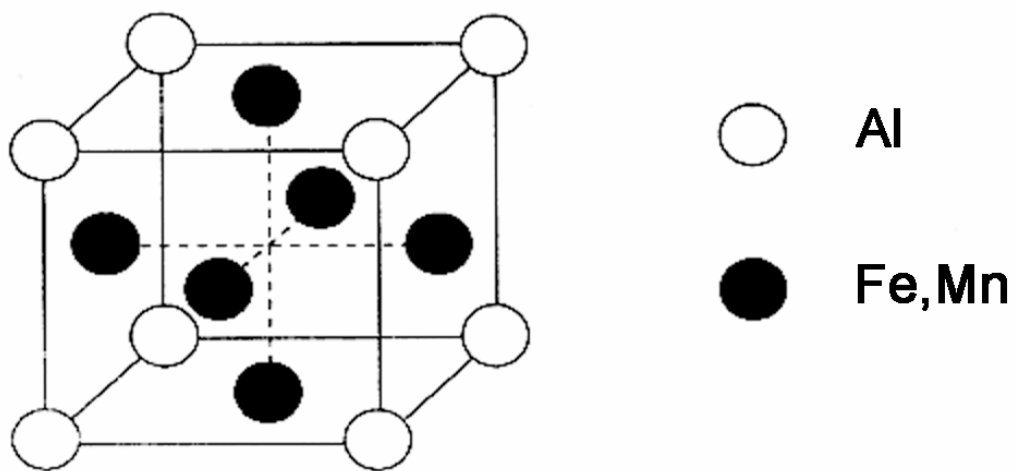


Figure 1.1(b)

Figure 1.1 (a)  $L'1_2$  crystal structure. (b)  $L1_2$  crystal structure.

# Chapter 2.

Phase Transitions in an

Fe-9Al-30Mn-2.0C Alloy



# Phase Transitions in an Fe-9Al-30Mn-2.0C Alloy

## Abstract

The as-quenched microstructure of the alloy was austenite phase containing fine  $(\text{Fe,Mn})_3\text{AlC}$  carbides. When the alloy was aged at 900 -1100°C and then quenched, both of large and extremely fine  $(\text{Fe,Mn})_3\text{AlC}$  carbides could be observed simultaneously within the austenite matrix. This feature has never been observed by other workers in the Fe-Al-Mn-C alloy systems before. In addition, the Al and Mn concentrations in the coarse  $(\text{Fe,Mn})_3\text{AlC}$  carbides formed on the grain boundaries were found to vary drastically with the aging temperature.



## 2-1 Introduction

Phase transitions in austenitic Fe-Al-Mn-C alloys, prepared by conventional casting process, have been studied by many workers [1-12]. In their studies, it is found that when an alloy with a chemical composition in the range of Fe-(6-11)wt.%Al-(26-34)wt.%Mn-(0.54-1.3)wt.%C was solution heat-treated and then quenched rapidly, the microstructure was single-phase austenite ( $\gamma$ ). After being aged at 500-750°C for moderate times, fine and coarse  $(\text{Fe,Mn})_3\text{AlC}$  carbides were found to precipitate coherently within the austenite matrix and heterogeneously on the austenite grain boundaries, respectively. Both of the fine and coarse  $(\text{Fe,Mn})_3\text{AlC}$  carbides have an  $L'1_2$  structure [1-6]. For convenience, the  $\kappa'$  carbide and  $\kappa$  carbide were used to represent the  $(\text{Fe,Mn})_3\text{AlC}$  carbide formed coherently within the austenitic matrix and heterogeneously on the  $\gamma/\gamma$  grain boundaries. With increasing the aging time within this temperature range, the coarse  $\kappa$  carbides grew into the adjacent austenite grains through a  $\gamma \rightarrow \gamma_0(\text{carbon-lack austenite}) + \kappa$  carbide reaction, a  $\gamma \rightarrow \alpha(\text{ferrite}) + \kappa$  carbide reaction, a  $\gamma \rightarrow \kappa$  carbide +  $\beta\text{-Mn}$  reaction, a  $\gamma \rightarrow \alpha + \kappa$  carbide +  $\beta\text{-Mn}$  reaction, or a  $\gamma \rightarrow \alpha + \beta\text{-Mn}$  reaction [4-9], depending on the chemical composition and aging temperature. Besides the extensive studies of the Fe-Al-Mn-C alloys with  $C \leq 1.3$  wt.%, the phase transitions in the conventionally prepared Fe-Al-Mn-C alloys with higher carbon

content have also been examined by several workers [10-12]. Based on their studies, it is obvious that the as-quenched microstructure of the Fe-(6-9)wt.%Al- (26-30.7)wt.%Mn-(1.5-2.8)wt.%C alloys was austenite phase containing fine  $\kappa'$  carbides [10,11]. This is quite different from that observed in the austenitic Fe-Al-Mn-C alloys with  $C \leq 1.3$  wt.% . It seems to imply that the carbon content may play an important role in the formation of fine  $\kappa'$  carbides within the austenite matrix during quenching. When the Fe-Al-Mn-C alloys with  $1.5 \leq C \leq 2.8$  wt.% were aged between 800 and 1200°C for longer times, the stable microstructure was found to be the mixture of (austenite phase +  $\kappa$  carbide) [10-12]. In the previous studies, it is clearly seen that most examinations of the Fe-Al-Mn-C alloys with higher carbon were only focused on the alloys at 800°C or above. Little information was available concerning the microstructural developments of the alloys at lower temperature. Therefore, the purpose of this work is an attempt to study the phase transitions in the Fe-9wt.%Al-30wt.%Mn-2.0wt.%C alloy heat-treated at 550-1200°C.

## 2-2 Experimental Procedure

The alloy, Fe-9wt.%Al-30wt.%Mn-2.0wt.%C, was prepared in a vacuum induction furnace by using 99.7% iron, 99.9% aluminum, 99.9% manganese and pure carbon powder. After being homogenized at 1250°C for 12 h under a controlled protective argon atmosphere, the ingot was hot-forged and then cold-rolled to a final thickness of 2.0 mm. The sheet was subsequently solution heat-treated at 1200°C for 2 h and rapidly quenched into room-temperature water. Aging processes were carefully performed at 550-1200°C for various times in a muffle furnace under a controlled protective argon atmosphere and then quenched.



Electron microscopy specimens were prepared by means of a double-jet electropolisher with an electrolyte of 60% acetic acid, 30% ethanol and 10% perchloric acid. The polishing temperature was kept in the range from -30°C to -15°C, and the current density was kept in the range from  $3.0 \times 10^4$  to  $4.0 \times 10^4$  A/m<sup>2</sup>. Electron microscopy was performed on a JEOL JEM-2000FX scanning transmission electron microscope (STEM) operating at 200 kV. This microscope was equipped with a Link ISIS 300 energy-dispersive X-ray

spectrometer (EDS) for chemical analysis. Quantitative analyses of elemental concentrations for Fe, Al and Mn were made with a Cliff-Lorimar Ratio Thin Section method.



## 2-3 Results and Discussion

Figure 2.1(a) is a bright-field (BF) electron micrograph of the as-quenched alloy, indicating that a high density of fine precipitates with a modulated structure was formed within the austenite matrix. Figure 2.1(b), a selected-area diffraction pattern (SADP), demonstrates that the fine precipitates are  $(\text{Fe,Mn})_3\text{AlC}$  carbides ( $\kappa'$  carbides) having an  $L'1_2$  structure [1-6,10-11]. Figure 2.1(c), a dark-field (DF) electron micrograph taken with the  $(100)_{\kappa'}$  superlattice reflection in  $[001]$  zone, reveals that the fine  $\kappa'$  carbides were formed along  $\langle 100 \rangle$  directions. This is consistent with the appearance of the satellites along  $\langle 100 \rangle$  reciprocal lattice directions in Figure 2.1(b). Accordingly, the as-quenched microstructure of the alloy was austenite phase containing fine  $\kappa'$  carbides. The fine  $\kappa'$  carbides were formed by spinodal decomposition during quenching. The result is similar to that reported by other workers in the as-quenched Fe-Al-Mn-C alloys with  $1.5 \leq C \leq 2.8$  wt.% [10-11].

When the as-quenched alloy was aged at  $550^\circ\text{C}$  for moderate times, the fine  $\kappa'$  carbides grew within the austenite matrix and a heterogeneous precipitation started to occur on the austenite grain boundaries. A typical microstructure is shown in Figure 2.2(a). Figure 2.2(b), an SADP taken from the coarse precipitate marked as "K" in Figure 2.2(a), indicates that the grain

boundary precipitate is also  $(\text{Fe,Mn})_3\text{AlC}$  carbide ( $\kappa$  carbide) having an  $L'1_2$ -type structure. After prolonged aging at  $550^\circ\text{C}$ , the coarse  $\kappa$  carbides grew into adjacent austenite grains through a  $\gamma \rightarrow \gamma_0$  (carbon-lack austenite) +  $\kappa$  carbide reaction. An example is shown in Figure 2.3(a), which is a BF electron micrograph of the alloy aged at  $550^\circ\text{C}$  for 32 h. With increasing the aging time at  $550^\circ\text{C}$ , the  $\gamma \rightarrow \gamma_0 + \kappa$  carbide reaction would proceed toward the whole austenite grains, as illustrated in Figure 2.3(b). In Figure 2.3(b), it is also seen that only the  $\kappa$  carbides could be observed within the  $\gamma_0$  phase.

TEM examinations indicated that the transition behavior could be preserved up to  $850^\circ\text{C}$ . However, when the alloy was aged at  $900^\circ\text{C}$  and then quenched, a high density of extremely fine precipitates could be detected within the remaining austenite matrix and within  $\gamma_0$  phase, as shown in Figure 2.4. Figure 2.4(a), a BF electron micrograph of the alloy aged at  $900^\circ\text{C}$  for 4 h and then quenched, clearly reveals that two types of  $\kappa'$  carbides can be observed within the austenite matrix; one is the larger  $\kappa'$  carbides (as indicated by arrows) which were existent at the aging temperature, and the other is the extremely fine  $\kappa'$  carbides which were formed during quenching from  $900^\circ\text{C}$ . Figure 2.4(b), an SADP taken from a region marked as "A" in Figure 2.4(a), reveals that satellite lying along  $\langle 100 \rangle$  reciprocal lattice directions about the (200) and (220) reflection spots could be observed. This indicates that the extremely fine  $\kappa'$

carbides having an  $L'1_2$  structure were formed by spinodal decomposition during quenching, which is similar to that observed in the as-quenched alloy. It is worthwhile to note that the presence of the large and extremely fine  $\kappa'$  carbides simultaneously within the austenite matrix has not previously been observed by other workers in the Fe-Al-Mn-C alloy systems before. Similarly, TEM examinations revealed that the presence of the coarse  $\kappa$  carbide and extremely fine  $\kappa'$  carbides could also be detected within the  $\gamma_0$  phase, as illustrated in Figures 2.4(c) and (d). Figure 2.4(e), an SADP taken from the coarse  $\kappa$  carbide marked as “K” in Figure 2.4(c), shows that the difference of the intensity between the (100) and (110) superlattice spots is only very slight. This is quite different from that taken from the coarse  $\kappa$  carbide in the alloy aged at 550°C (Figure 2.2(b)).

Progressively higher temperature aging and quenching experiments indicated that the grain boundary precipitation of  $\kappa$  carbides could exist up to 1100°C. However, as the aging temperature was increased to 1150°C, only fine  $\kappa'$  carbides were formed within the austenite matrix and no evidence of grain boundary precipitation could be detected, as shown in Figure 2.5. This indicates that the microstructure of the alloy present at 1150°C or above should be single-phase austenite.

On the basis of the preceding results, it is evident that both of the large and extremely fine  $\kappa'$  carbides could be observed simultaneously within the austenite matrix in the alloy aged at 900°C and then quenched. This feature has never been observed by other workers in the Fe-Al-Mn-C alloy systems before. In the previous studies of the Fe-Al-Mn-C alloy with C  $\leq$  1.3wt.% [1-9], it is seen that the as-quenched microstructure was single-phase austenite. Therefore, it is reasonable to propose that although the presence of the large  $\kappa'$  carbides, the carbon concentration within the remaining austenite matrix in the alloy at 900°C was still greater than 1.3 wt.%, which may lead to the formation of extremely fine  $\kappa'$  carbides by spinodal decomposition during quenching. As the above proposition, it is also anticipated that in spite of the preipitation of coarse  $\kappa$  carbides on the grain boundaries, the carbon concentration within the  $\gamma_0$  phase was still enough to result in the formation of the extremely fine  $\kappa'$  carbides during quenching from 900°C, as observed in Figures 2.4(c) and (d).

In the previous studies, it was reported that when the austenitic Fe-Al-Mn-C alloys were aged at 550-750°C for longer times, the coarse  $\kappa$  carbides started to occur on the grain boundaries. The crystal structure of the coarse  $\kappa$  carbide was L'1<sub>2</sub>, which is the same as that of the fine  $\kappa'$  carbides formed within the austenite matrix [4,6,10]. According to the structure factor  $|F_{hkl}|$  calculations [10], it is seen that the difference between  $|F_{100}|$  and  $|F_{110}|$  for



the  $(\text{Fe,Mn})_3\text{AlC}$  carbide having an  $L'1_2$  structure is  $2f_c$ , where  $f_c$  is the electron scattering factor for carbon atom. Since  $2f_c$  represents a very large difference, the actual intensity of (100) spot should be much stronger than that of (110) spot [10]. In the present study, it is clearly seen in Figure 2.2(b) that the intensity of the superlattice (100) spot is indeed much stronger than the (110) spot, indicating that the coarse  $\kappa$  carbide formed in the alloy aged at  $550^\circ\text{C}$  has an  $L'1_2$  structure. However, the difference of the intensity between these two superlattice spots is only very slight for the coarse  $\kappa$  carbide in the alloy aged at  $900^\circ\text{C}$ . In order to clarify this feature, an STEM-EDS study was undertaken. Figures 2.6(a) through (c) represent three typical EDS spectra taken from the coarse  $\kappa$  carbide in the alloy aged at 550, 750 and  $900^\circ\text{C}$ , respectively. The average concentrations of substitutional alloying elements obtained by analyzing a number of EDS spectra are listed in Table 2.1. In Figure 2.6 and Table 2.1, it is obvious that the Al concentration of the  $\kappa$  carbide increased drastically with the aging temperature, and the reverse result was obtained for the Mn content. This result is similar to that examined by the present workers in the Fe-10.1wt.%Al-28.6wt.%Mn-0.46wt.%C alloy [13]. Furthermore, in the previous studies [11,12], it was found that in the  $\kappa$  carbide, the C concentration was always less than 20 at.% of the stoichiometric  $(\text{Fe,Mn})_3\text{AlC}$  composition and the C concentration would decrease markedly as Al concentration

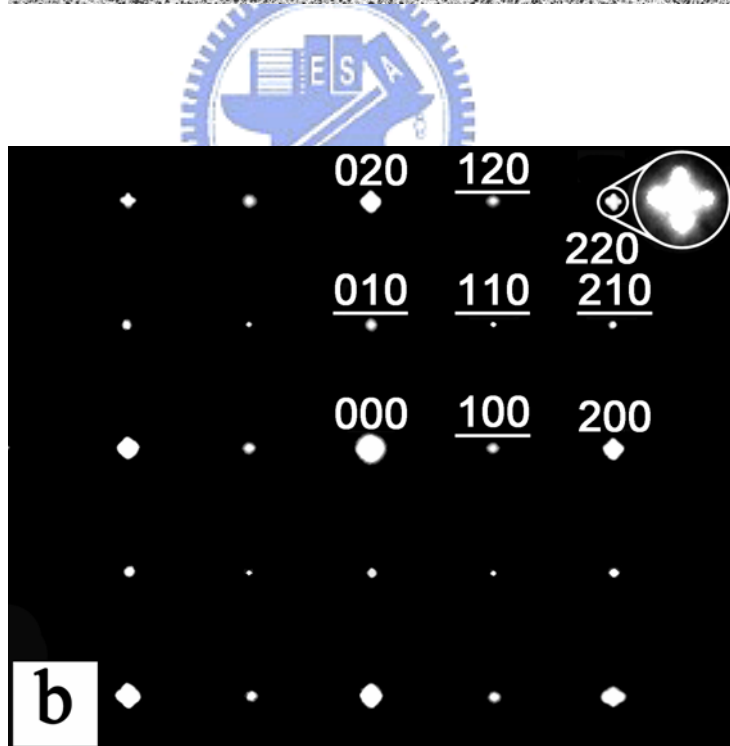
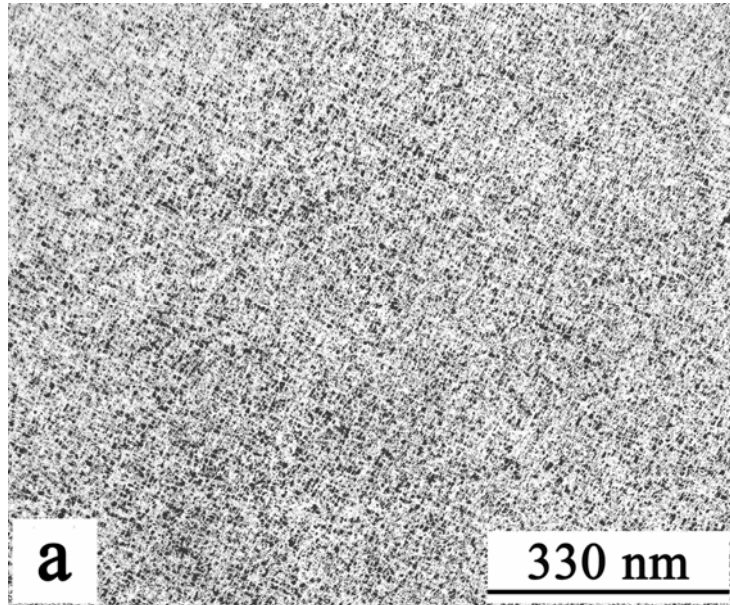
increased. For example, the C concentration in the  $\kappa$  carbide was 15.6 at.% with 15.9 at.% Al and only 13.1 at.% with 18.7 at.% Al [11]. The EDS examinations revealed that when the present alloy was aged at 900°C, the Al concentration in the  $\kappa$  carbide was increased up to 19.8 at.%. Therefore, it is plausible to suggest that owing to the increase of the Al concentration, the C concentration in the  $\kappa$  carbide would be greatly lowered, which would significantly decrease the difference of the intensity between the (100) and (110) superlattice spots. Finally, it is worthwhile to point out that EDS with a thick-window detector used in the present study is limited to detect the elements of atomic number 11 or above, therefore, C cannot be examined. Obviously, in order to further understand the transition behaviors in the Fe-Al-Mn-C alloys, much more work is needed.

## 2-4 Conclusions

The as-quenched microstructure of the Fe-9wt.%Al-30wt.%Mn- 2.0wt.%C alloy was austenite phase containing fine  $\kappa'$  carbides. The fine  $\kappa'$  carbides having an  $L'1_2$  structure were formed by spinodal decomposition during quenching. When the as-quenched alloy was aged at 550-1100°C for moderate times, the fine  $\kappa'$  carbides grew within the austenite matrix and a  $\gamma \rightarrow \gamma_0 + \kappa$  carbide reaction started to occur on the austenite grain boundaries. The Al and Mn concentrations in the  $\kappa$  carbide would vary drastically with the aging temperature. In addition, when the alloy was aged at 900°C and then quenched, extremely fine  $(\text{Fe,Mn})_3\text{AlC}$  carbides could be formed within the remaining austenite matrix and within  $\gamma_0$  phase by spinodal decomposition during quenching.

## References

- [1] K.H. Han, J.C. Yoon, W.K. Choo, Scripta Metall. 20 (1986) 33.
- [2] K. Sato, K. Tagawa, Y. Inoue, Scripta Metall. 22 (1988) 899.
- [3] C.N. Hwang, T.F. Liu, Scripta Mater. 36 (1997) 853.
- [4] C.N. Hwang, C.Y. Chao, T.F. Liu, Scripta Metall. 28 (1993) 263.
- [5] C.Y. Chao, C.N. Hwang T.F. Liu, Scripta Metall. 28 (1993) 109.
- [6] W.K. Choo, J.H. Kim, J.C. Yoon, Acta Mater. 45 (1997) 4877.
- [7] I.S. Kalashnikov, O. Acselrad, A. Shalkevich, J. Mater. Processing Technology 136 (2003) 72.
- [8] G.S. Krivonogov, M.F. Alekseyenko, G.G. Solov'yeva, Fiz. Metal. Metalloved. 39 (1975) 86.
- [9] K. Sato, K. Tagawa, Y. Inoue, Metal. Trans. A 21 (1990) 5.
- [10] K. Ishida, H. Othani, N. Satoh, R. Kainuma, T. Nishizawa, ISIJ International 30 (1990) 680.
- [11] Y. Kimura, K. Handa, K. Hayashi, Y. Mishima, Intermetallics 12 (2004) 607.
- [12] Y. Kimura, K. Hayashi, K. Handa, Y. Mishima, Mater. Sci. Eng. A 329-331 (2002) 680.
- [13] C.C. Wu, J.S. Chou, T.F. Liu, Metal. Trans. A 22 (1991) 2265.



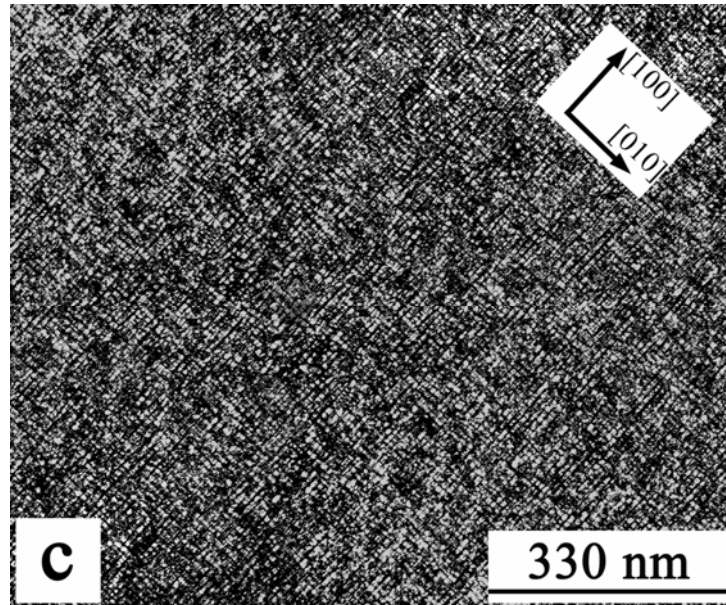


Figure 2.1 Transmission electron micrographs of the as-quenched alloy: (a) BF, (b) an SADP taken from the mixed region of austenite matrix and fine  $\kappa'$  carbides. The foil normal is [001] ( $hkl$ : austenite matrix;  $\underline{hkl}$ :  $\kappa'$  carbide), and (c) DF obtained by use of the  $(100)_{\kappa'}$  superlattice reflection in the [001] zone.

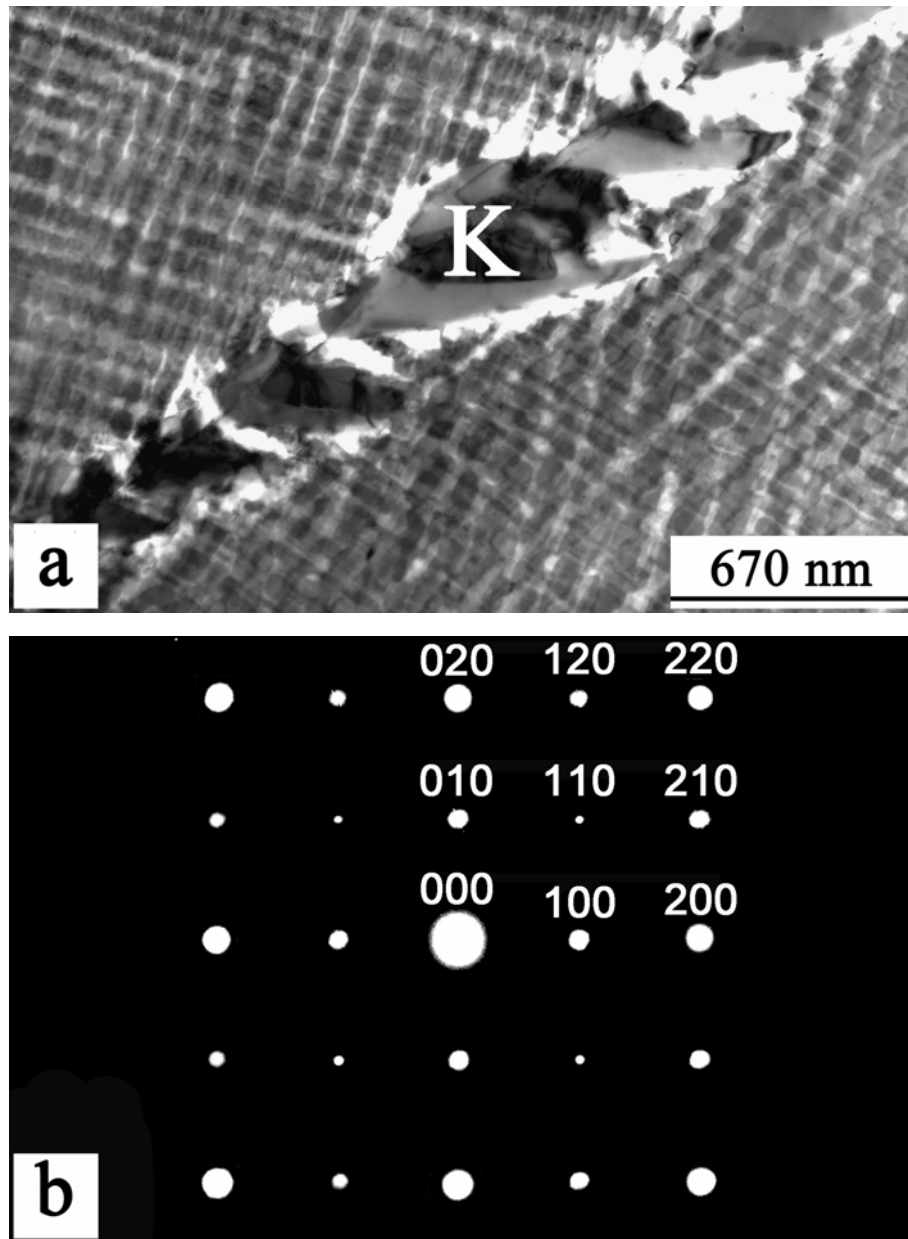


Figure 2.2 Transmission electron micrographs of the alloy aged at 550°C for 12 h: (a) BF, and (b) an SADP taken from the  $\kappa$  carbide marked as “K” in (a).

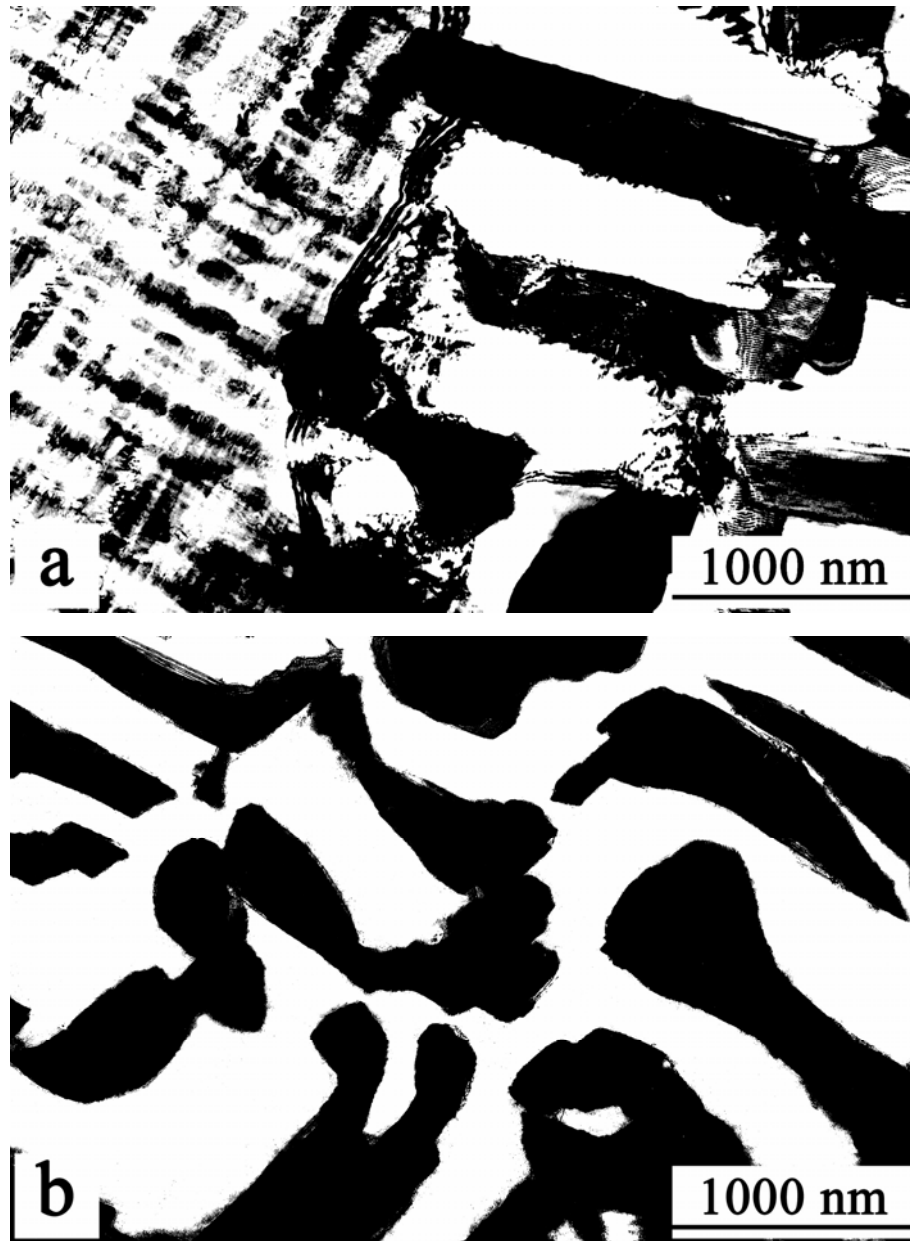
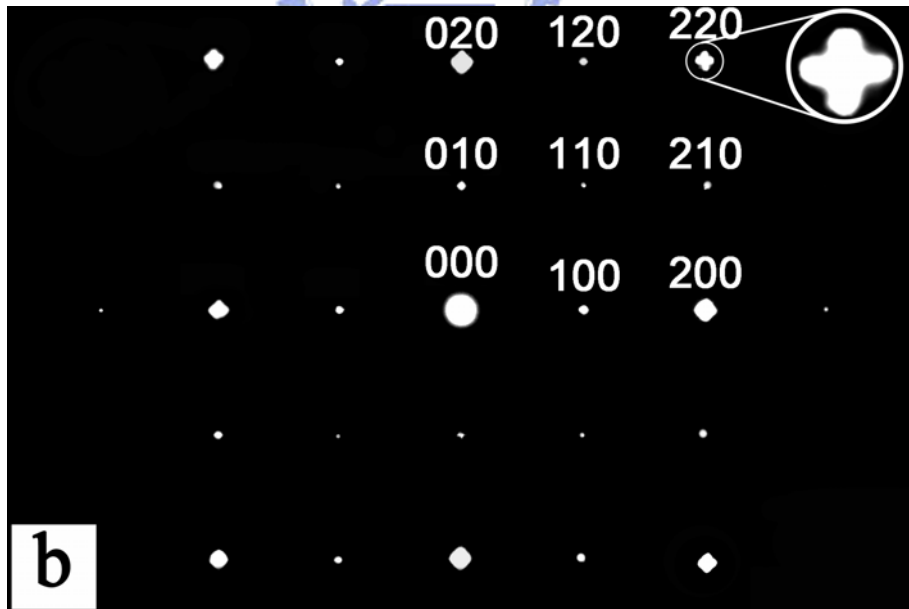
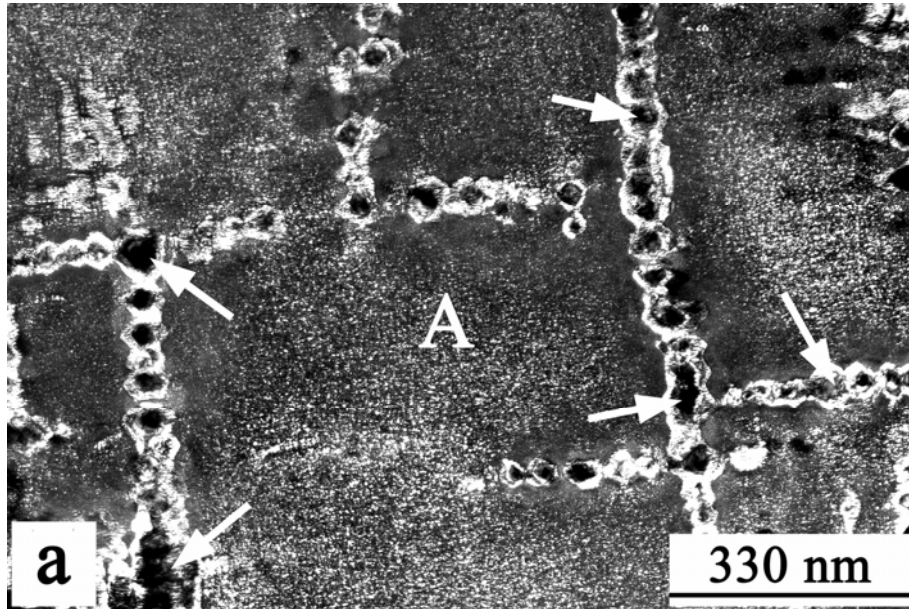
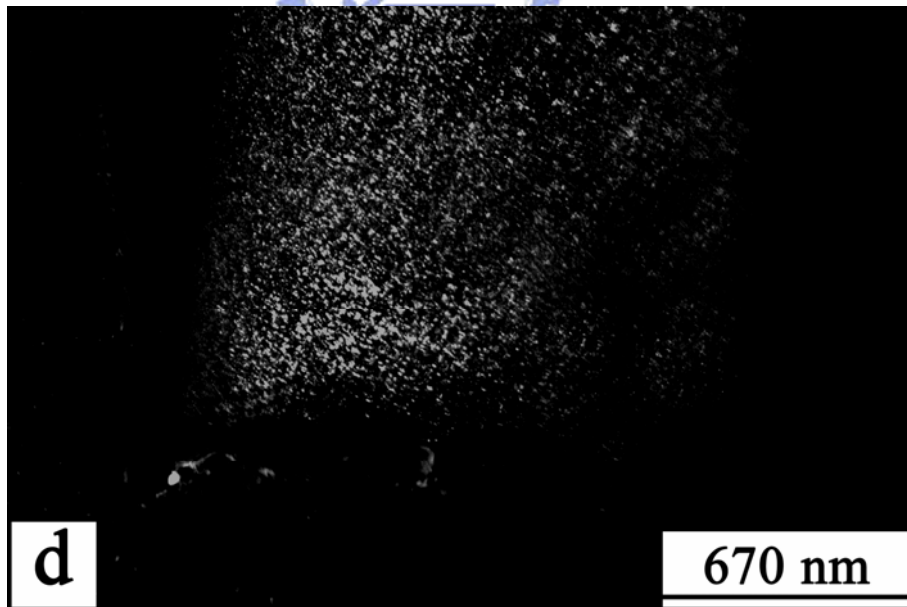
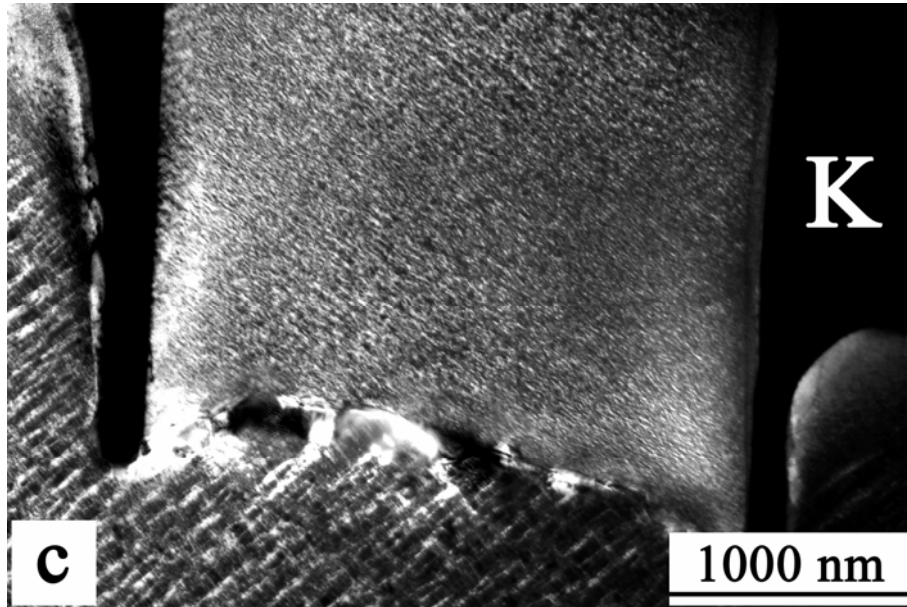


Figure 2.3 BF electron micrographs of the alloy aged at 550°C for (a) 32 h, and (b) 48 h.







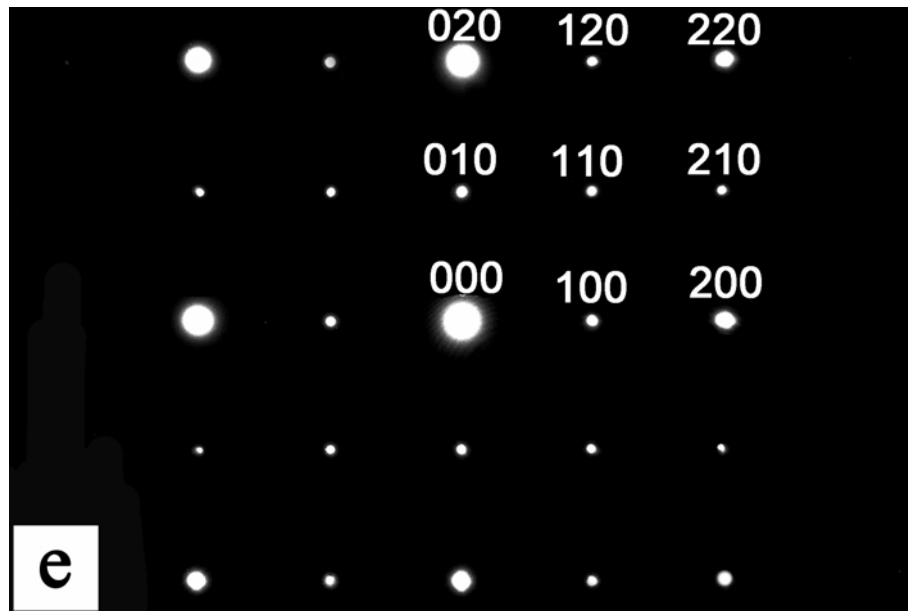


Figure 2.4 Transmission electron micrographs of the alloy aged at 900°C for 4 h. (a) BF, (b) an SADP taken from the region marked as “A” in (a), (c) BF, (d) (100) $\kappa'$  DF, and (e) an SADP taken from the coarse  $\kappa$  carbide marked as “K” in (c).

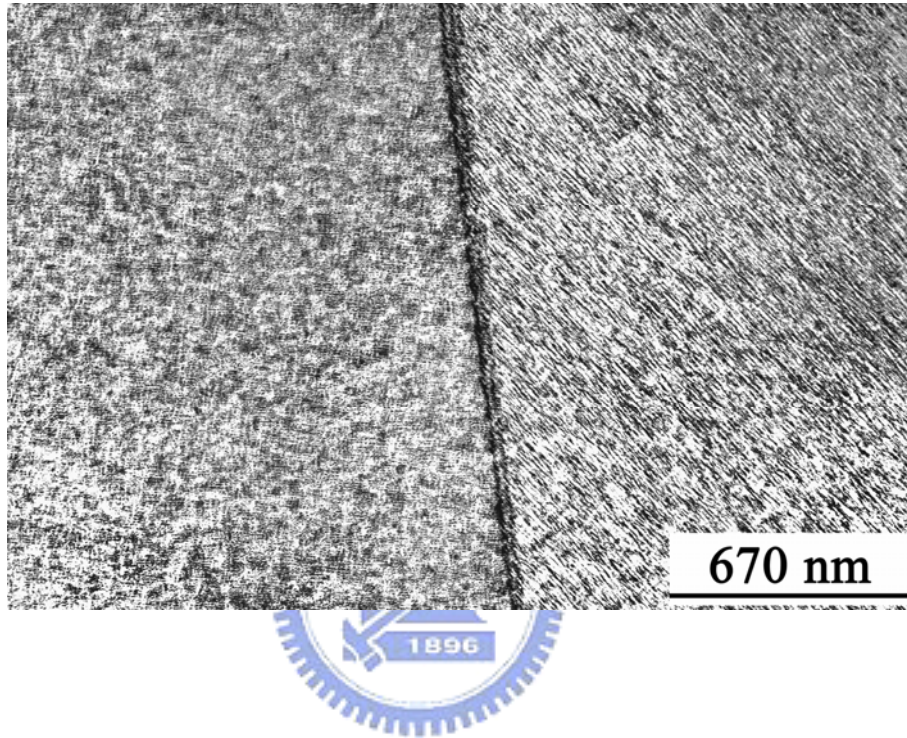
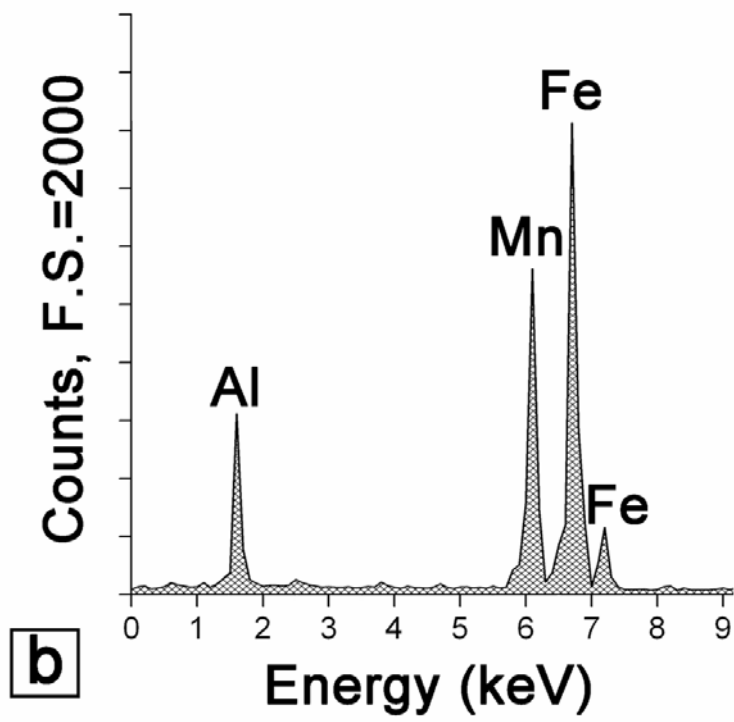
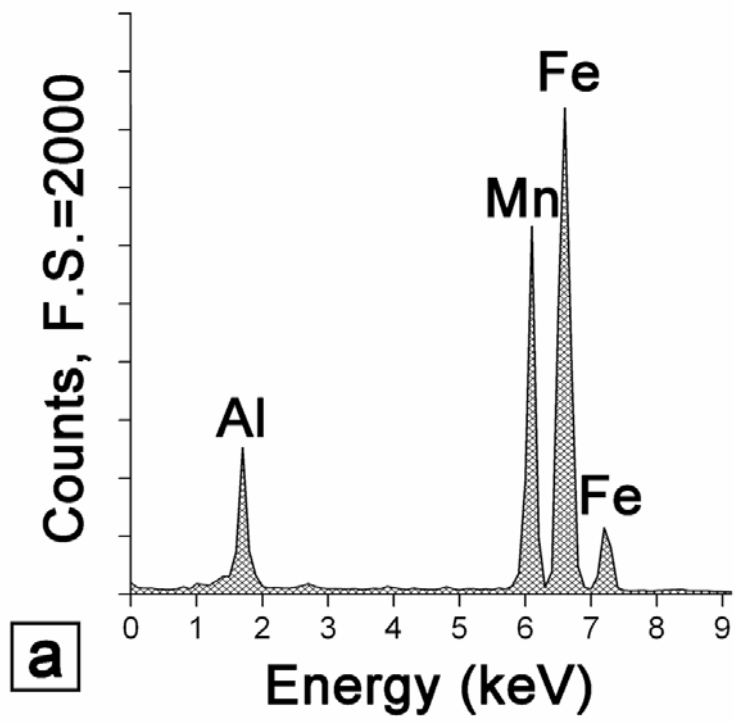


Figure 2.5 BF electron micrograph of the alloy aged at 1150°C for 1 h.



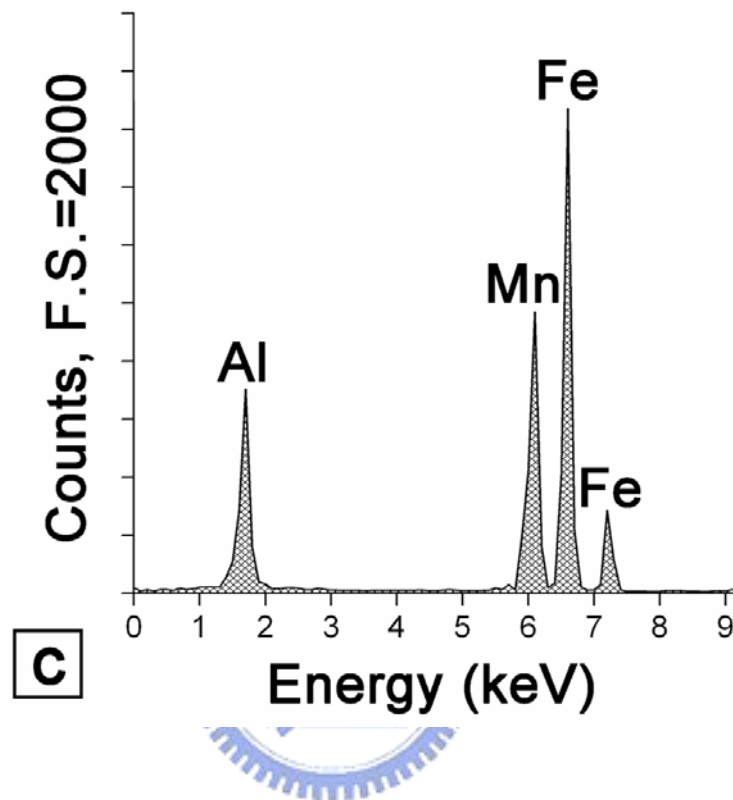
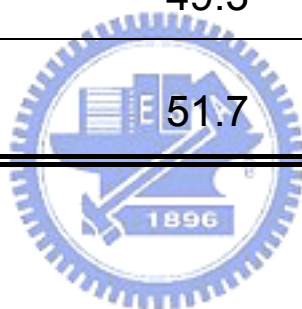


Figure 2.6 Three typical EDS spectra taken from the coarse  $\kappa$  carbide in the alloy aged at (a) 550°C, (b) 750°C, and 900°C, respectively.

Table 2.1 Chemical compositions of the  $\kappa$  carbide revealed by EDS.

Aging Temperature	Chemical Composition (at.%)		
	Fe	Al	Mn
550°C	47.2	14.2	38.6
750°C	49.3	16.5	34.2
900°C	51.7	19.8	28.5



# Chapter 3.

## Mechanical Properties of an Fe-9Al-30Mn-2.0C Alloy





# Mechanical Properties of an Fe-9Al-30Mn-2.0C Alloy

## Abstract

The microstructures and mechanical properties of an Fe-9wt.%Al-30wt.%Mn-2.0wt.%C alloy in the as-quenched condition and after aged at 750°C have been studied. The as-quenched microstructure of the Fe-9wt.%Al-30wt.%Mn-2.0wt.%C alloy was austenite ( $\gamma$ ) phase containing fine  $(\text{Fe,Mn})_3\text{AlC}$  carbides ( $\kappa'$  carbides). When the alloy was aged at 750°C for moderate times, the fine  $(\text{Fe,Mn})_3\text{AlC}$  carbides grew within the austenite matrix and a  $\gamma + \kappa' \rightarrow \gamma + \text{coarse } (\text{Fe,Mn})_3\text{AlC carbide } (\kappa \text{ carbide})$  reaction occurred on the grain boundaries. The mixture of ( $\gamma + \kappa$  carbides) had a lamellar structure. With increasing aging time, the  $\gamma + \kappa' \rightarrow \gamma + \kappa$  reaction proceeded toward the inside of the  $\gamma$  grains. After prolonged aged at 750°C, the final microstructure of the Fe-9wt.%Al-30wt.%Mn-2.0wt.%C alloy was  $\gamma/\kappa$  lamellar structure. Tensile tests revealed that the optimal combination of mechanical strength and ductility of the alloy was the as-quenched specimen which had good ultimate tensile strength (UTS) of 1060 MPa with an excellent 57% elongation. When the

as-quenched alloy was aged at 750°C for 3-96 h, both the tensile strength and ductility were significantly decreased. Interestingly, both of the mechanical strength and ductility of the as-quenched specimen were much better than those of the aged specimens. It is worthwhile to note that the mechanical properties of the austenitic Fe-Al-Mn-C alloys with C > 1.3wt.% in the as-quenched condition have never been investigated by other workers before. In addition, the  $\gamma/\kappa$  lamellar structure of the aged specimens could not improve the tensile ductility because sub-cracks initiated at coarsened  $\kappa$  carbides and linked up to trigger cleavage.



### 3-1 Introduction

The microstructures and mechanical properties of the austenitic Fe-Al-Mn-C alloys have been extensively studied by many researchers [1-15]. In their studies, it is found that when an alloy with a chemical composition in the range of Fe-(9-11)%Al-(26-34)%Mn-(0.54-1.3)%C (all compositions are in wt.% throughout otherwise specified) was solution heat-treated and then rapidly quenched, the microstructure was single-phase austenite ( $\gamma$ ). After being aged at 500-800°C for moderate times, fine  $(\text{Fe,Mn})_3\text{AlC}$  carbides started to precipitate coherently within the austenite matrix [1-12]. The  $(\text{Fe,Mn})_3\text{AlC}$  carbides has an ordered  $L'1_2$ -type structure [1-12]. Owing to the precipitation of fine  $(\text{Fe,Mn})_3\text{AlC}$  carbides within the austenite matrix, the strength of the alloy was remarkably increased without significant loss in ductility. After prolonged aging at 500-800°C,  $(\text{Fe,Mn})_3\text{AlC}$  carbides were found to precipitate not only coherently within the austenite matrix, but also heterogeneously on the  $\gamma/\gamma'$  grain boundaries in the form of coarser particles [6-9]. For convenience, the  $\kappa'$  carbide and  $\kappa$  carbide were used to represent the  $(\text{Fe,Mn})_3\text{AlC}$  carbide formed coherently within the austenitic matrix and heterogeneously on the  $\gamma/\gamma'$  grain boundaries. With increasing the aging time within this temperature range, the coarse  $\kappa$  carbides grew into the adjacent austenite grains through a  $\gamma \rightarrow \gamma_0$  (carbon-lack austenite) +  $\kappa$  carbide reaction, a  $\gamma \rightarrow \alpha$  (ferrite) +  $\kappa$  carbide

reaction, a  $\gamma \rightarrow \kappa$  carbide +  $\beta$ -Mn reaction, a  $\gamma \rightarrow \alpha + \kappa$  carbide +  $\beta$ -Mn reaction, or a  $\gamma \rightarrow \alpha + \beta$ -Mn reaction [7-12] depending on the chemical composition and aging temperature. However, the grain boundary precipitates resulted in the embrittlement of the austenitic Fe-Al-Mn-C alloys [6,7,12]. For example, in the previous studies in the Fe-7.8%Al-30%Mn-1.3%C alloy [7], it was reported by Choo et al. that the as-quenched Fe-7.8%Al-30%Mn-1.3%C alloy exhibited yield strength (YS) 475 MPa with 57% elongation. Optimal mechanical properties (YS 1080 MPa and ultimate tensile strength (UTS) 1120 MPa) could be attained when the alloy was aged at 550°C for about 100 h; however, when the alloy was further aged at 550°C, both YS and UTS decreased with prolonged aging time and the alloy finally became extremely brittle.

Besides the extensive studies of the Fe-Al-Mn-C alloys with  $C \leq 1.3\%$ , the microstructures of the conventionally prepared austenitic Fe-Al-Mn-C alloys with higher carbon content ( $C > 1.3\%$ ) have also been examined by several workers [5,13-15]. In their studies, it is obvious that the as-quenched microstructure of the Fe-(7-12)%Al-(29.3-30.5)%Mn-(1.5-2.6)%C alloys was austenite phase containing fine  $\kappa'$  carbides [5,13,14]. This is quite different from that observed in the austenitic Fe-Al-Mn-C alloys with  $C \leq 1.3\%$ . When the Fe-Al-Mn-C alloys with  $1.5 \leq C \leq 2.6\%$  were aged between 550 and 900°C for

moderate times, fine  $(\text{Fe,Mn})_3\text{AlC}$  carbides grew within  $\gamma$  matrix and coarse  $(\text{Fe,Mn})_3\text{AlC}$  carbides started to occur on grain boundaries. After prolonged aging, the coarse  $\kappa$  carbides grew into the adjacent  $\gamma$  grains through a  $\gamma + \kappa' \rightarrow \gamma + \kappa$  reaction. The mixture of  $(\gamma + \kappa \text{ carbide})$  had a lamellar structure [14]. With increasing the aging time, the  $\gamma + \kappa' \rightarrow \gamma + \kappa$  reaction would proceed toward the whole  $\gamma$  grains. Consequently, the stable microstructure was a lamellar product of  $\gamma + \kappa$  [14].

In contrast to the studies of the microstructures, information concerning the mechanical properties of the austenitic Fe-Al-Mn-C alloys with  $\text{C} > 1.3\%$  is very deficient. We are aware of only one article [14], in which the mechanical properties of the austenitic Fe-Al-Mn-C alloys with higher C content were examined. In 2004, Kimura et al. reported that in the furnace-cooled condition, the Fe-15at.%Al-26at.%Mn-8at.%C (Fe-8.5%Al-29.5%Mn-2.0%C, in wt.%) alloy exhibited UTS around 550 MPa and almost zero elongation; in order to improve the ductility, the alloy was solution heat-treated at  $1100^\circ\text{C}$  followed by water quenched, and subsequently aged at  $800^\circ\text{C}$  for 120 h. After the heat treatment, the microstructure was a lamellar product of  $\gamma + \kappa$ . By forming the  $\gamma/\kappa$  lamellar structure, the elongation could be improved to be about 10% with YS 675 MPa and UTS 1020 MPa [14]. Besides this, little information was available

concerning the mechanical properties of the Fe-Al-Mn-C alloys with C > 1.3%.


Therefore, the purpose of this work is to study the mechanical properties of the

Fe-9%Al-30%Mn-2.0%C alloy.



## 3-2 Experimental Procedure

The alloy, Fe-9wt.%Al-30wt.%Mn-2.0wt.%C, was prepared in a vacuum induction furnace by using 99.7% iron, 99.9% aluminum, 99.9% manganese and pure carbon powder. After being homogenized at 1250°C for 12 h under a controlled protective argon atmosphere, the ingot was hot-forged and then cold-rolled to a final thickness of 8.0 mm. The sheet was subsequently solution heat-treated at 1200°C for 2 h and rapidly quenched into room-temperature water. Aging processes were carefully performed at 750°C for 3-96 h in a muffle furnace under a controlled protective argon atmosphere and then quenched.



Optical microscopy, scanning electron microscopy (SEM, JEOL JSM-6500FX) and transmission electron microscopy (TEM) were carried out to examine the microstructural characterization. TEM specimens were prepared by means of a double-jet electropolisher with an electrolyte of 60% acetic acid, 30% ethanol and 10% perchloric acid. The polishing temperature was kept in the range from -30°C to -15°C, and the current density was kept in the range from  $3.0 \times 10^4$  to  $4.0 \times 10^4$  A/m<sup>2</sup>. Transmission electron microscopy examination was performed on a JEOL JEM-2000FX scanning transmission electron microscope (STEM) operating at 200 kV.

Tensile tests were carried out with an Instron tensile test machine at room

temperature with a strain rate of  $5 \times 10^{-4} \text{ s}^{-1}$ . Tensile test specimens are plates having the gauge length of 25 mm, 6.25 mm width and 6.4 mm thickness. After tensile test, SEM analysis was carried out to examine the fracture surface and the free surface contiguous to the fracture surface.





### 3-3 Results and Discussion

Figure 3.1(a) is an optical micrograph of the alloy in the as-quenched condition, exhibiting  $\gamma$  grains with annealing twins. Figure 3.1(b), a selected-area diffraction pattern (SADP), reveals that satellite lying along  $\langle 100 \rangle$  reciprocal lattice directions about the (200) and (220) reflection spots could be observed. This indicates that the extremely fine precipitates are  $(\text{Fe,Mn})_3\text{AlC}$  carbides ( $\kappa'$  carbides) having an  $L'1_2$  structure, which were formed by spinodal decomposition during quenching [1-11]. Figure 3.1(c), a dark-field (DF) electron micrograph taken with the  $(100)_{\kappa'}$  superlattice reflection in [001] zone, reveals that the fine  $\kappa'$  carbides were formed along  $\langle 100 \rangle$  directions. This is consistent with the appearance of the satellites along  $\langle 100 \rangle$  reciprocal lattice directions in Figure 3.1(b). Accordingly, the as-quenched microstructure of the alloy was  $\gamma$  phase containing fine  $\kappa'$  carbides. The fine  $\kappa'$  carbides were formed by spinodal decomposition during quenching. The result is similar to that reported by the previous workers in the as-quenched Fe-Al-Mn-C alloys with  $1.5 \leq C \leq 2.8\%$  [13,14].

When the as-quenched alloy was aged at  $750^\circ\text{C}$  for moderate times, the fine  $\kappa'$  carbides grew within the  $\gamma$  matrix and a heterogeneous precipitation of  $\gamma/\kappa$  lamellar structure started to occur on the  $\gamma/\gamma$  grain boundaries. A typical

microstructure is shown in Figure 3.2(a). Figure 3.2(a) is a SEM micrograph of the typical microstructures of the alloy aged at 750°C for 24 h, shows that the fine  $\kappa'$  carbides grew within the  $\gamma$  matrix (as indicated by “ $\gamma + \kappa'$ ”) and the  $\gamma/\kappa$  lamellar structure occurred on the  $\gamma/\gamma$  grain boundaries (as indicated by “ $\gamma + \kappa$ ”). After prolonged aging at 750°C, the coarse  $\kappa$  carbides grew into adjacent  $\gamma$  grains through a  $\gamma + \kappa'$  carbide  $\rightarrow \gamma + \kappa$  carbide reaction proceeding toward the whole austenite grains and the stable microstructure was found to be a lamellar product of  $\gamma + \kappa$ , as illustrated in Figure 3.2(b). In Figure 3.2(b), it is also seen that only the stable  $\gamma/\kappa$  lamellar structure could be observed, which is similar to that observed by Y. Kimura et al. in the Fe-15at.%Al-26at.%Mn-8at.%C (Fe-8.5%Al-29.5%Mn-2.0%C, in wt.%) alloy after aged at 800°C for 120 h [14].

To evaluate the effect of lamellar microstructure on the mechanical properties, especially on the ductility, tensile tests were conducted on the alloy in the as-quenched condition and aged at 750°C for various times. The results are shown in Figure 3.3. In Figure 3, it is seen that the UTS value of the as-quenched specimen is 1060 MPa with an excellent 57% elongation; whereas, it is worthy mentioning that the UTS and YS values of all the aged specimens were slightly decreased and their elongations were drastically dropped to be about 3-5%.

In order to clarify the fracture behaviors of the alloy, SEM fracture and free surface analyses were undertaken on the as-quenched and 24 h aged tensile test specimens, respectively. Figure 3.4(a), a fractograph of the as-quenched specimen, reveals that the as-quenched specimen has a ductile dimple fracture surface. Figure 3.4(b), SEM micrograph taken from the free surface contiguous to the fracture surface of the as-quenched tensile test specimen, shows that slip bands generated over the specimen. The structure shows a high resistance to crack propagation and exhibits self stabilization under deformation (as indicated by arrows). From the observation of microstructure, fracture surface and free surface, it seems to imply that the fine  $\kappa'$  carbides which are coherent with the  $\gamma$  matrix were likely strengthening the as-quenched specimen and the ductility is not sacrificed during the fine  $\kappa'$  carbides strengthening the matrix. This explains the tensile test result of the as-quenched specimen, which reveals good strength (UTS 1060MPa) with an excellent 57% elongation.

On the contrary, after aged for 24 h, the specimen fractured without almost any deformation and exhibited a cleavage fracture surface (Figure 3.4(c)). Figure 3.4(d) shows that isolated sub-cracks were observed only at coarse  $\kappa$  carbides within the  $\gamma/\kappa$  lamellar structure contiguous to fracture surface and no crack could be observed in un-reacted  $\gamma + \kappa'$  region. The coarse  $\kappa$  carbides of a

$\gamma/\kappa$  lamellar colony have a much higher stiffness than their companion of  $\gamma$  and were broken into two when they could not accommodate the slip deformation of  $\gamma$ . This allowed the slip to go on inside the  $\gamma/\kappa$  lamellar colony and acted as a void nucleation mechanism for the discontinuities produced by the breakage of coarse  $\kappa$  carbides. The voids grew assisted by plastic deformation until they linked up and became flaws able to initiate and trigger cleavage. Therefore, it seems that the homogeneous distribution of lamellar coarse  $\kappa$  carbides could not be beneficial to the ductility of the Fe-9%Al-30%Mn-2.0%C alloy.



## 3-4 Conclusions

The mechanical properties of the conventionally prepared Fe-9%Al-30%Mn-2.0%C alloy have been examined in the present study. The results obtained are as follows:

(1) The optimal combination of mechanical strength and ductility was the as-quenched specimen which had good UTS of 1060 MPa with an excellent 57% elongation. Both the mechanical strength and ductility of the as-quenched specimen were superior to those of the specimens aged at 750°C for 3-96 h. It is noted that the mechanical properties of the as-quenched Fe-Al-Mn-C alloys with  $C > 1.3\%$  have never been investigated by other workers before.

(2) The  $\gamma/\kappa$  lamellar microstructure of the aged specimens could not improve tensile ductility because sub-cracks initiated at coarsened  $\kappa$  carbides of the  $\gamma/\kappa$  lamellar colony and linked up to trigger cleavage.

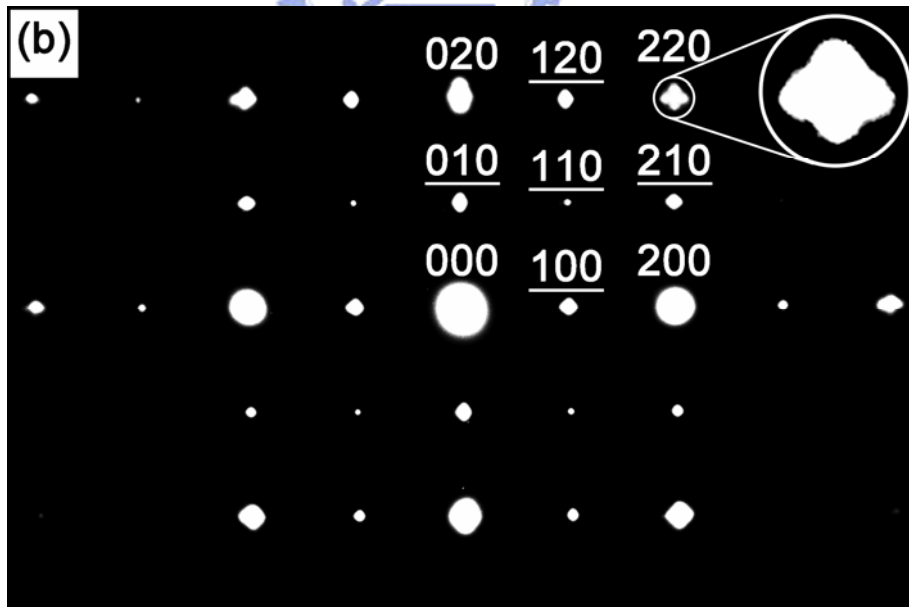
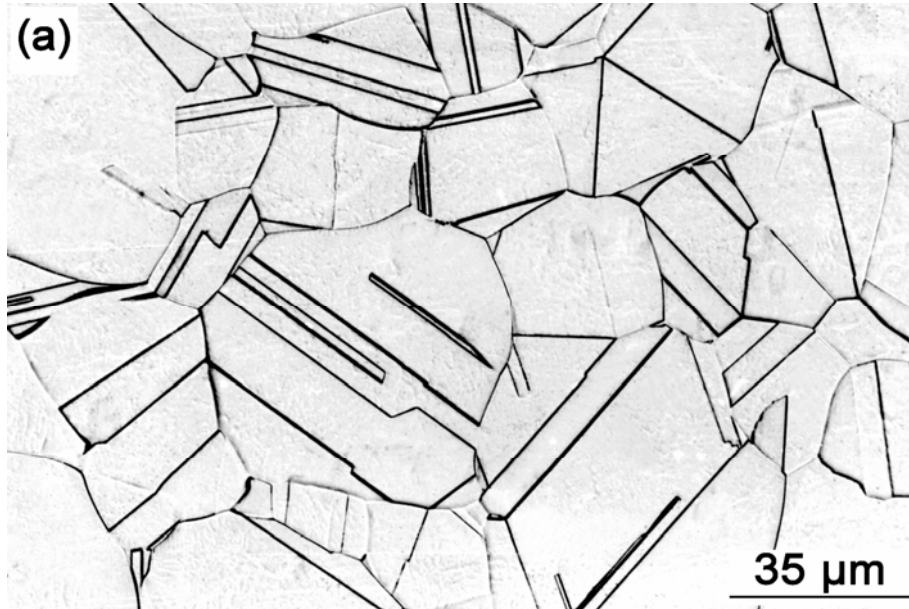
## References

- [1] K. Sato, K. Tagawa, Y. Inoue, *Scripta Metall.* 22 (1988) 899.
- [2] K.H. Han, J.C. Yoon, W.K. Choo, *Scripta Metall.* 20 (1986) 33.
- [3] Y. Ikarashi, K. Sato, T. Yamazaki, Y. Inoue, M. Yamanaka, *J. Mater. Sci. Letters* 11 (1992) 733.
- [4] C.N. Hwang, T.F. Liu, *Scripta Materialia* 36 (1997) 853.
- [5] C.Y. Chao, L.K. Hwang, T.F. Liu, *Scripta Metall.* 29 (1993) 647.
- [6] K. Sato, K. Tagawa, Y. Inoue, *Mater. Sci. Eng. A* 111 (1989) 45.
- [7] W.K. Choo, J.H. Kim, J.C. Yoo, *Acta Mater.* 45 (1997) 4877.
- [8] C.Y. Chao, C.N. Hwang, T.F. Liu, *Scripta Metall.* 28 (1993) 109.
- [9] C.N. Hwang, C.Y. Chao, T.F. Liu, *Scripta Metall.* 28 (1993) 263.
- [10] K. Sato, K. Tagawa, Y. Inoue, *Metall. Trans A* 21 (1990) 5.
- [11] G.S. Krivonogov, M.F. Alekseyenko, G.G. Solov'yeva, *Phys. Met. Metall.* 39 (1975) 775.
- [12] I.S. Kalashnikov, O. Acselrad, A. Shalkevich, L.D. Chumakova, L.C. Pereira, *J. Mater. Processing Techno.* 136 (2003) 72.
- [13] K. Ishida, H. Ohtani, N. Satoh, R. Kainuma, T. Nishizawa, *ISIJ Inter.* 30 (1990) 680.
- [14] Y. Kimura, K. Handa, K. Hayashi, Y. Mishima, *Intermetallics* 12 (2004)

607.

- [15] Y. Kimura, K. Hayashi, K. Handa, Y. Mishima, Mater. Sci. Eng. A 329-331  
(2002) 680.







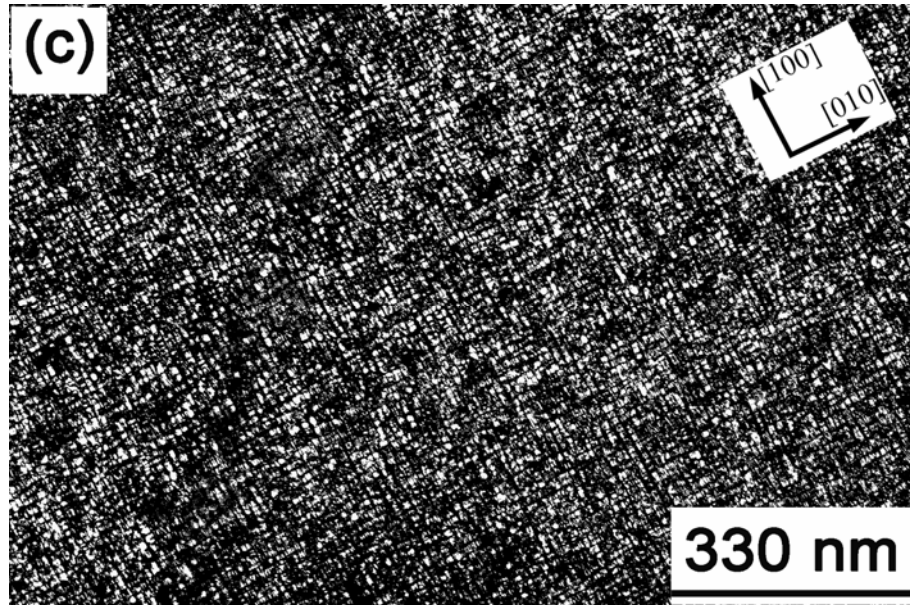


Figure 3.1 Micrographs of the Fe-9%Al-30%Mn-2.0% C alloy in the as-quenched condition. (a) an optical micrograph, (b) a selected-area diffraction pattern taken from the mixed region of austenite matrix and fine  $\kappa'$  carbides. The foil normal is [001] ( $hkl$ : austenite matrix;  $\underline{hkl}$ :  $\kappa'$  carbide), and (c) a dark-field (DF) electron micrograph taken by  $(100)_{\kappa'}$  superlattice reflection in [001] zone.

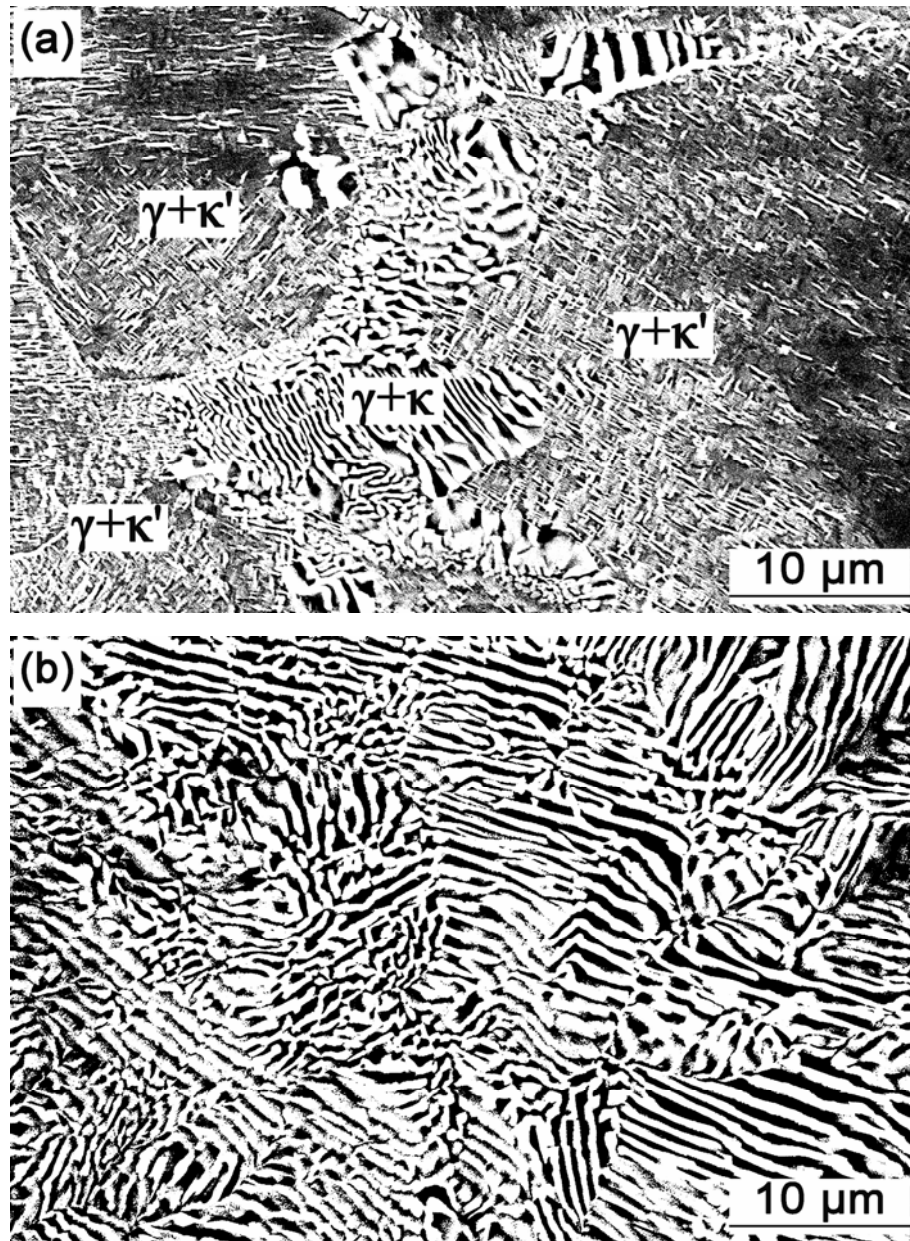


Figure 3.2 SEM micrographs of the alloy aged at 750°C for (a) 24 h, and (b) 96 h.

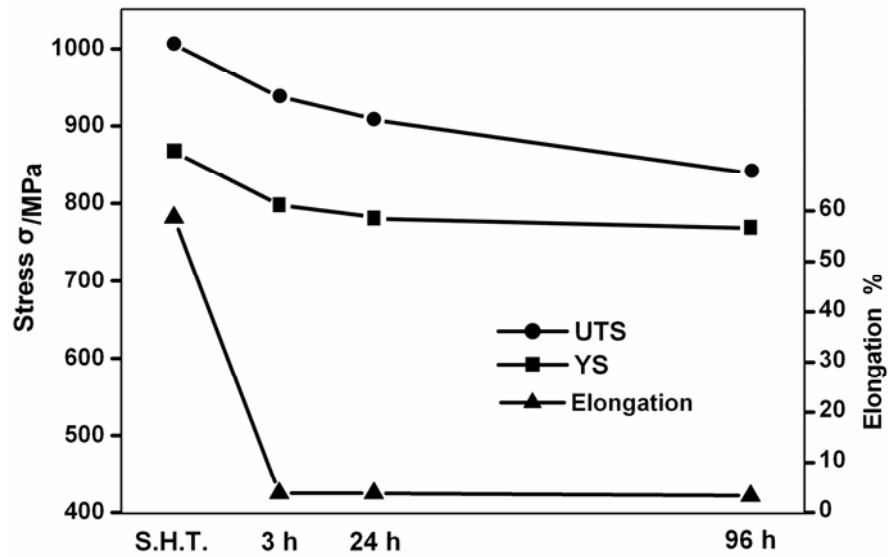
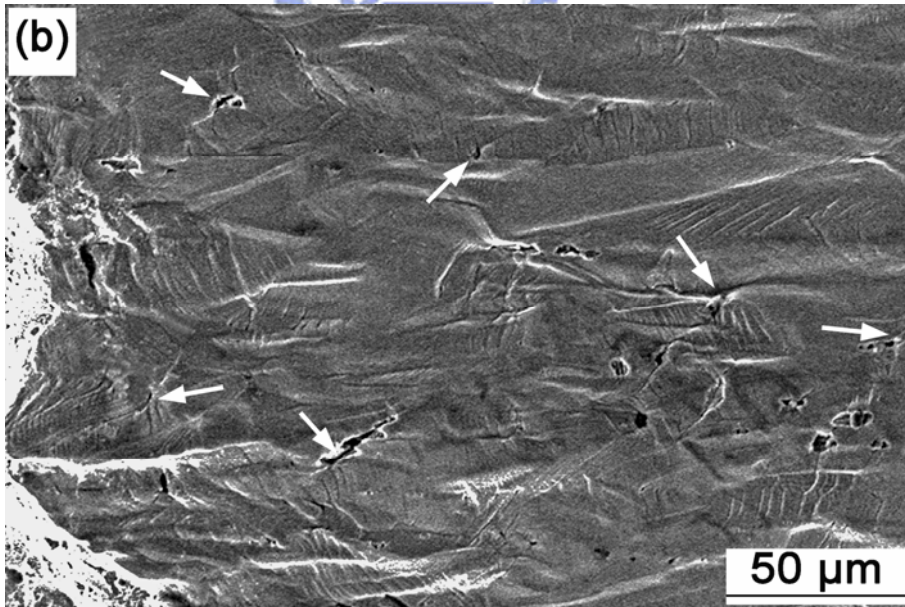
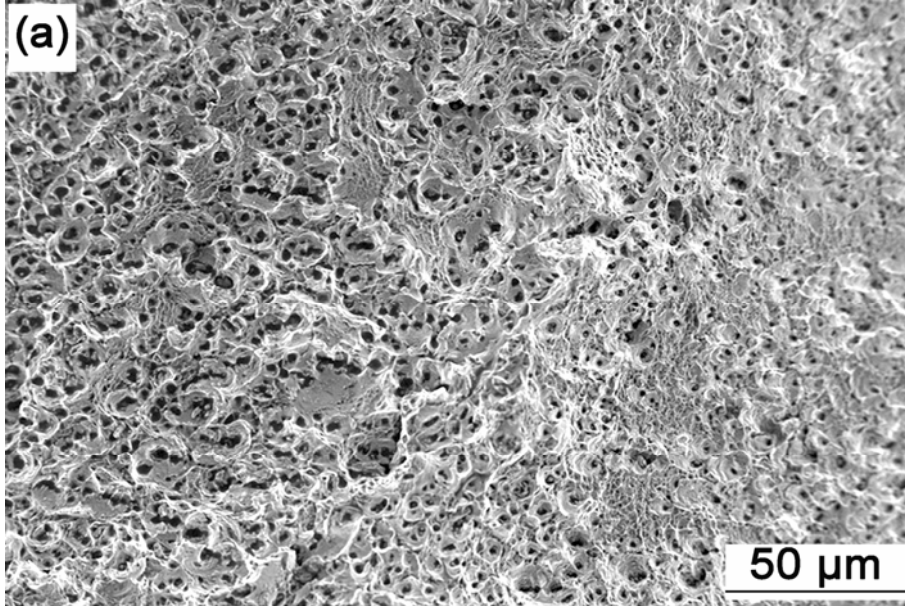


Figure 3.3 Tensile test results of the alloy in the as-quenched condition and after aged at 750°C for various times.



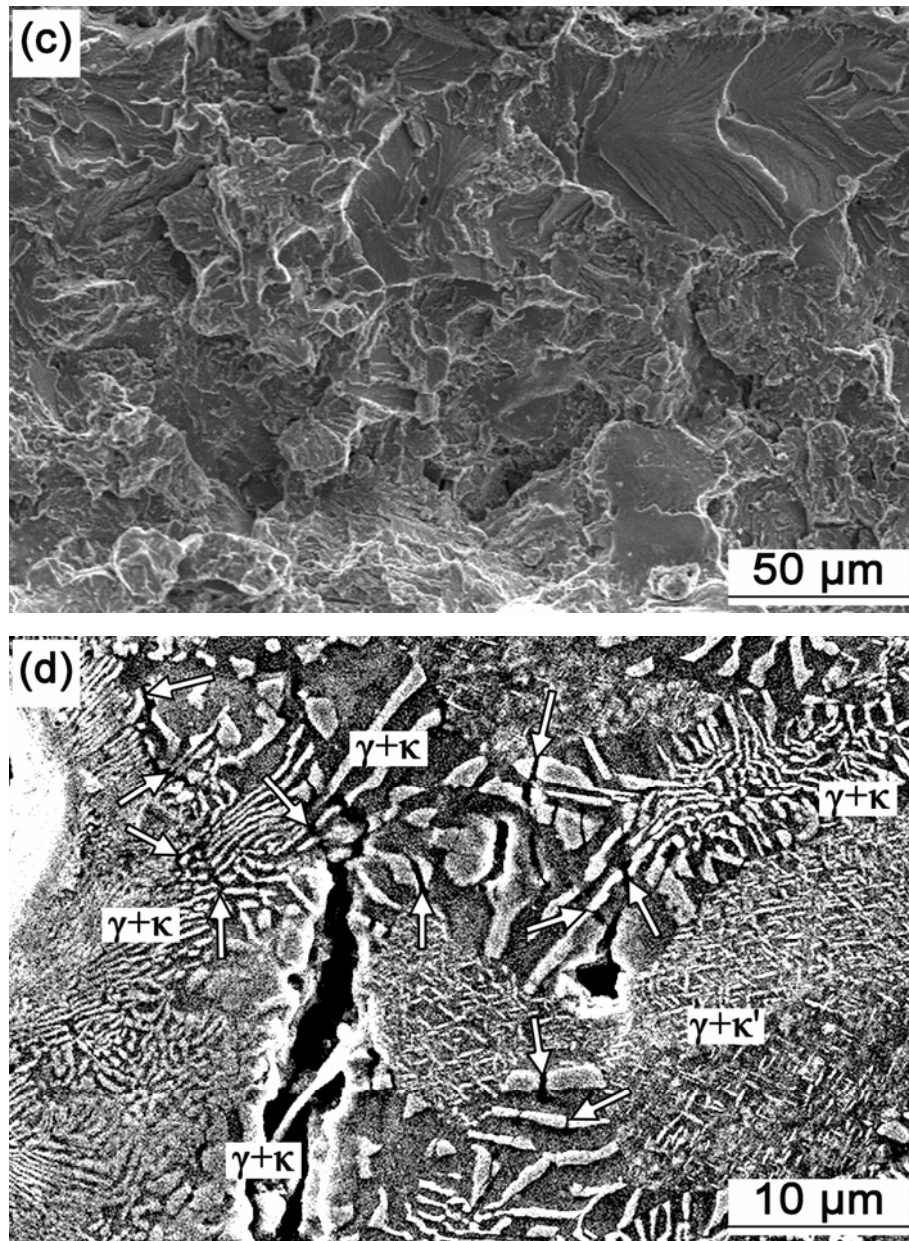


Figure 3.4 SEM micrographs of the fractured specimen. (a) and (b), fracture and free surfaces of the as-quenched specimen, respectively. (c) and (d), fracture and free surfaces of the specimen aged at 750°C for 24 h, respectively.

# Chapter 4.

## Mechanical Properties of an Fe-9Al-30Mn-1.0C Alloy



# Mechanical Properties of an Fe-9Al-30Mn-1.0C Alloy

## Abstract

The as-quenched microstructure of the Fe-9wt.%Al-30wt.%Mn-1.0wt.%C alloy was a single austenite ( $\gamma$ ) phase. When the alloy was aged at 625°C for short times, fine  $(\text{Fe,Mn})_3\text{AlC}$  carbides ( $\kappa'$  carbides) were observed to precipitate within the  $\gamma$  matrix, but not on the  $\gamma/\gamma$  grain boundaries. However, after prolonged aging at 625°C, the fine  $(\text{Fe,Mn})_3\text{AlC}$  carbides grew within the  $\gamma$  matrix and a  $\gamma + \kappa' \rightarrow \gamma + \text{coarse } (\text{Fe,Mn})_3\text{AlC carbide } (\kappa \text{ carbide})$  reaction occurred on the grain boundaries. The mixture of ( $\gamma + \kappa$  carbides) had a lamellar structure. Subsequently, with increasing aging time, the  $\gamma + \kappa' \rightarrow \gamma + \kappa$  reaction proceeded toward the inside of the  $\gamma$  grains. Tensile tests revealed that the optimal combination of mechanical strength with ductility of the alloy was the 24 h aged specimen which had good ultimate tensile strength (UTS) of 1023 MPa and an excellent 44% elongation. After prolonged aging, both the tensile strength and ductility were slightly decreased. However, although the  $\gamma/\kappa$

lamellar structure occurred on the  $\gamma/\gamma$  grain boundaries after aged at 625 °C for 96 h, the present alloy still exhibited good 28% elongation. Obviously, this result is quite different from that observed in the Fe-9wt.%Al-30wt.%Mn-2.0wt.%C alloy with similar structure (after aged at 750°C for 3 h).





## 4-1 Introduction

In previous literatures, the microstructure and mechanical properties of the conventionally prepared austenitic Fe-Al-Mn-C alloys have been extensively studied by many researchers [1-20]. In their studies, it is found that when an alloy with a chemical composition in the range of Fe-(9-11)%Al-(26-34)%Mn-(0.54-1.3)%C (all compositions are in wt.% throughout otherwise specified) was solution heat-treated and then quenched rapidly, the microstructure was single-phase austenite ( $\gamma$ ). After being aged at 500-800°C for moderate times, fine  $(\text{Fe,Mn})_3\text{AlC}$  carbides started to precipitate coherently within the  $\gamma$  matrix [1-12]. The  $(\text{Fe,Mn})_3\text{AlC}$  carbides has an ordered  $L'_{12}$ -type structure [1-12]. Owing to the precipitation of fine  $(\text{Fe,Mn})_3\text{AlC}$  carbides within the  $\gamma$  matrix, the strength of the alloy was remarkably increased without significant loss in ductility. After prolonged aging at 500-800°C,  $(\text{Fe,Mn})_3\text{AlC}$  carbides were found to precipitate not only coherently within the  $\gamma$  matrix, but also heterogeneously on the  $\gamma/\gamma$  grain boundaries in the form of coarser particles [6-9]. For convenience, the  $\kappa'$  carbide and  $\kappa$  carbide were used to represent the  $(\text{Fe,Mn})_3\text{AlC}$  carbide formed coherently within the  $\gamma$  matrix and heterogeneously on the  $\gamma/\gamma$  grain boundaries. With increasing the aging time within this temperature range, the coarse  $\kappa$  carbides grew into the adjacent  $\gamma$  grains through a  $\gamma \rightarrow \gamma_0$  (carbon-lack austenite) +  $\kappa$  carbide reaction, a  $\gamma \rightarrow \alpha$

(ferrite) +  $\kappa$  carbide reaction, a  $\gamma \rightarrow \kappa$  carbide +  $\beta$ -Mn reaction, a  $\gamma \rightarrow \alpha + \kappa$  carbide +  $\beta$ -Mn reaction, or a  $\gamma \rightarrow \alpha + \beta$ -Mn reaction [7-12] depending on the chemical composition and aging temperature. However, the grain boundary precipitation resulted in the embrittlement of the austenitic Fe-Al-Mn-C alloys [6,7,12]. For example, in the previous studies [7], it was reported by Choo et al. that the as-quenched Fe-7.8%Al-30%Mn-1.3%C alloy exhibited yield strength (YS) 475 MPa and 57% elongation. Optimal mechanical properties (YS 1080 MPa, ultimate tensile strength (UTS) 1120 MPa and about 31.5% elongation) could be attained when the alloy was aged at 550°C for about 100 h; however, when the alloy was further aged at 550°C, both YS and UTS decreased with increasing aging time and the alloy finally became extremely brittle, which was due to the formation of the grain boundary lamellar colonies composed of discontinuously coarsened  $\kappa$  carbides and transformed  $\alpha$  (ferrite) phases.

Besides the extensive studies of the Fe-Al-Mn-C alloys with  $C \leq 1.3\%$ , the microstructures of the conventionally prepared austenitic Fe-Al-Mn-C alloys with higher carbon content ( $C > 1.3\%$ ) have also been examined by several workers [5,13-15]. Based on their studies, it is obvious that the as-quenched microstructure of the Fe-(7-12)%Al-(29.3-30.5)%Mn-(1.5-2.6)%C alloys was  $\gamma$  phase containing fine  $\kappa'$  carbides [5,13,14]. This is quite different from that observed in the austenitic Fe-Al-Mn-C alloys with  $C \leq 1.3\%$ . When the

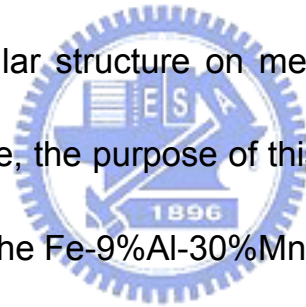
Fe-Al-Mn-C alloys with  $1.5 \leq C \leq 2.6\%$  were aged between 550 and 900°C for moderate times, fine  $(\text{Fe,Mn})_3\text{AlC}$  carbides grew within  $\gamma$  matrix and coarse  $(\text{Fe,Mn})_3\text{AlC}$  carbides started to occur on grain boundaries. After prolonged aging, the coarse  $\kappa$  carbides grew into the adjacent  $\gamma$  grains through a  $\gamma + \kappa' \rightarrow \gamma + \kappa$  reaction. The mixture of ( $\gamma + \kappa$  carbide) had a lamellar structure [14]. With increasing the aging time, the  $\gamma + \kappa' \rightarrow \gamma + \kappa$  reaction would proceed toward the whole  $\gamma$  grains. Consequently, the stable microstructure was a lamellar product of  $\gamma + \kappa$  [14].

In contrast to the studies of the microstructures, information concerning the mechanical properties in the conventionally prepared Fe-Al-Mn-C alloys with higher C content is very deficient. We are aware of only one article [14], in which the mechanical properties of the austenitic Fe-Al-Mn-C alloys with higher C content were examined. In 2004, Kimura et al. reported that in the furnace-cooled condition, the Fe-15at.%Al-26at.%Mn-8at.%C (Fe-8.5%Al-29.5%Mn-2.0%C, in wt.%) alloy exhibited UTS around 550 MPa and almost zero ductility; in order to improve the ductility, the alloy was solution heat-treated at 1100°C for 1 h followed by water quenched, and subsequently aged at 800°C for 120 h. It was observed that the  $\gamma/\kappa$  lamellar structure was formed in the alloy after the heat treatment. By forming the  $\gamma/\kappa$  lamellar structure, the elongation could be improved to be about 10% with YS 675 MPa

and UTS 1020 MPa. Beside this, little information was available concerning the mechanical properties of the FeAlMnC alloys with higher C ( $C > 1.3\%$ ) content.

However, different result was observed in our previous study concerning the mechanical properties of the Fe-9%Al-30%Mn-2.0%C alloy [16], in which we found that the  $\gamma/\kappa$  lamellar microstructure of the aged specimens could not improve tensile ductility because sub-cracks initiated at coarsened  $\kappa$  carbides of the  $\gamma/\kappa$  lamellar colony and linked up to trigger cleavage.

Obviously, much more work is needed to clarify the microstructural influence of the  $\gamma/\kappa$  lamellar structure on mechanical properties of austenitic FeAlMnC alloys. Therefore, the purpose of this work is an attempt to study the mechanical properties of the Fe-9%Al-30%Mn-1.0%C alloy.



## 4-2 Experimental Procedure

The Fe-9wt.%Al-30wt.%Mn-1.0wt.%C alloy was prepared in a vacuum induction furnace by using 99.7% iron, 99.9% aluminum, 99.9% manganese and pure carbon powder. After being homogenized at 1250°C for 12 h under a controlled protective argon atmosphere, the ingot was hot-forged and then cold-rolled to a final thickness of 2.0 mm. The sheet was subsequently solution heat-treated at 1200°C for 2 h and rapidly quenched into room-temperature water. Aging processes were carefully performed at 625°C for various times in a muffle furnace under a controlled protective argon atmosphere and then quenched.



Optical microscopy, scanning electron microscopy (SEM, JEOL JSM-6500FX) and transmission electron microscopy (TEM) were used to carry out microstructural characterization. TEM specimens were prepared by means of a double-jet electropolisher with an electrolyte of 60% acetic acid, 30% ethanol and 10% perchloric acid. The polishing temperature was kept in the range from -30°C to -15°C, and the current density was kept in the range from  $3.0 \times 10^4$  to  $4.0 \times 10^4$  A/m<sup>2</sup>. Transmission electron microscopy was performed on a JEOL-2000FX scanning transmission electron microscope (STEM) operating at 200 kV.

Tensile tests were carried out with an Instron tensile test machine at room temperature with a strain rate of  $5 \times 10^{-4} \text{ s}^{-1}$ . Tensile test specimens are plates having the gauge length of 25 mm, 6.25 mm width and 6.4 mm thickness. After tensile test, SEM analysis was carried out to examine the fracture surface and the free surface in the vicinity of fracture surface.



## 4-3 Results and Discussion

An optical micrograph of the as-quenched alloy is shown in Figure 4.1. It reveals austenite grains with annealing twins. Transmission electron microscopy examinations indicated that no precipitates were formed within the austenite matrix in the as-quenched alloy.

Figure 4.2(a) shows a bright-field (BF) electron micrograph of the alloy aged at 625°C for 6 h, revealing that fine precipitates with a modulated structure were formed within the austenite matrix. Figure 4.2(b), a selected-area diffraction pattern (SADP) taken from a mixed region covering the austenite matrix and fine precipitates, demonstrates that the fine precipitates are  $(\text{Fe,Mn})_3\text{AlC}$  carbides ( $\kappa'$ -carbide) having an  $L'1_2$ -type structure [2,17-20]. Figure 4.2(c) is a dark-field (DF) electron micrograph taken with the  $(100)_{\kappa'\text{-carbide}}$  superlattice reflection in the  $[001]$  zone, indicating that these  $(\text{Fe,Mn})_3\text{AlC}$  carbides were formed along  $\langle 100 \rangle$  direction. This observation is similar to that observed by other workers in the aged Fe-Al-Mn-C alloys [1-12]. Transmission electron microscopy examinations indicated that no grain boundary precipitates could be observed in the alloy aged at 625°C for less than 12 h. However, after prolonged aging at 625°C, some coarse precipitates started to appear on the grain boundaries. A typical microstructure is illustrated

in Figure 4.3, which is a BF electron micrograph of the alloy aged at 625°C for 24 h. Analyses by SADPs showed that the coarse precipitates on the grain boundary are also  $(\text{Fe,Mn})_3\text{AlC}$  carbides ( $\kappa$ -carbides). With continued aging at 625°C, the  $\kappa$ -carbides grew into the adjacent austenite grains, as shown in Figure 4.4. Figure 4.4(a) is a SEM micrograph of the alloy aged at 625°C for 96 h, showing that the fine  $\kappa'$  carbides grew within the  $\gamma$  matrix (as indicated by “ $\gamma + \kappa'$ ”) and the  $\gamma/\kappa$  lamellar structure occurred on the  $\gamma/\gamma$  grain boundaries (as indicated by “ $\gamma + \kappa$ ”). Transmission electron microscopy of thin foils indicated that only the  $\gamma/\kappa$  lamellar structure could be observed to occur on the grain boundaries in the alloy aged at 625°C for 96h, as shown in Figures 4.4(b) and (c). Figure 4.4(b) is a typical microstructure of the alloy aged at 625°C for 96 h. Figure 4.4(c), an SADP taken from the coarse  $\kappa$  precipitate marked as “K” in 4.4(b) and its surrounding austenite phase, indicates that the grain boundary precipitate is also  $(\text{Fe,Mn})_3\text{AlC}$  carbide ( $\kappa$  carbide) having an  $L'_{12}$ -type structure.

To evaluate the effect of the  $\gamma/\kappa$  lamellar structure on the mechanical properties, especially on the ductility, tensile tests were conducted on the alloy in the as-quenched condition and aged at 625°C for various times. The results are shown in Figure 4.5. In Figure 4.5, it is seen that the UTS and YS values of the as-quenched specimen are 896 and 733 MPa, respectively, with an excellent 62% elongation. Besides, the high maximum UTS and YS of the



present alloy can be attained by aging for 24 h; the maximum UTS and YS are 1023 and 978 MPa, respectively, whereas it maintains a good 44% elongation. After prolonged aging at 625°C for longer times, both the strength and elongation of the present alloy were slightly decreased. However, it is worthy noting that the present alloy still exhibited good 28% elongation even through it was aged at 625°C for 96 h.

In order to clarify the fracture behaviors of the alloy, SEM fracture and free surface analyses were undertaken on the 24 h and 96 h aged tensile test specimens, respectively. Figure 4.6(a), a fractograph of the 24 h aged specimen, reveals that the 24 h aged specimen has a ductile dimple fracture surface. Figure 4.6(b), SEM micrograph taken from the free surface contiguous to the fracture surface of the 24 h aged tensile test specimen, shows that slip bands generated over the specimen. The structure shows a high resistance to crack propagation and exhibits self stabilization under deformation. From the observations of microstructure, fracture surface and free surface, it seems to imply that the fine  $\kappa'$  carbides which are coherent with the austenitic matrix are likely strengthening the 24 h aged specimen. The ductility is not sacrificed during the fine  $\kappa'$  carbides strengthening the matrix. This explains the tensile test result of the 24 h aged specimen, which reveals good strength (UTS 1023MPa) with an excellent 44% elongation.

Although the  $\gamma/\kappa$  lamellar structure occurred on the  $\gamma/\gamma$  grain boundaries after aged at 625°C for 96 h (as shown in Figure 4.4), the present alloy still exhibited good 28% elongation. SEM fracture and free surface analyses indicate that the 96 h aged specimen reveals a ductile-type fracture behavior, as shown in Figures 4.7(a) and (b). In Figure 4.7(a), it is seen that the 96 h aged specimen has a ductile dimple fracture surface although some micro-cracks can be observed on the grain boundaries. Figure 4.7(b) shows the ductile-type structure with slip band generation over the specimen, which is similar to that observed in Figure 4.6(b). Accordingly, it seems that the microstructural effect of the  $\gamma/\kappa$  lamellar structure on mechanical properties of the present Fe-9%Al-30%Mn-1.0%C alloy was insignificant. This result is different from that observed in the Fe-9%Al-30%Mn-2.0%C alloy, in which it was observed that all aged specimens with the  $\gamma/\kappa$  lamellar structure on grain boundaries were embrittled. In order to clarify the discrepancy, the area fractions of the  $\gamma/\kappa$  lamellar structure in the aged specimens were calculated by using an image processing software. The result is shown in Table 1. Table 1 shows that the area fraction of the  $\gamma/\kappa$  lamellar structure in the Fe-9%Al-30%Mn-1.0%C alloy after aged at 625°C for 96 h is 8.5% and that in the Fe-9%Al-30%Mn-2.0C alloy after aged at 750°C for 3 h is 19.3%. Evidently, higher area fraction of the  $\gamma/\kappa$  lamellar structure results in the embrittlement of

the austenitic Fe-Al-Mn-C alloys.



## 4-4 Conclusions

The microstructural effect on the mechanical properties of the austenitic Fe-9Al-30Mn-1.0C alloy, prepared by conventional casting process, have been studied. The results obtained are as follows:

(1) In as-quenched condition, the microstructure of the alloy is a single  $\gamma$  phase.

When the as-quenched alloy was aged at 625°C for short times, fine  $\kappa'$  carbides were found to precipitate within the  $\gamma$  matrix, but not on the grain boundaries. After prolonged aging at 625°C, coarse  $\kappa$  carbides started to appear on the grain boundaries. Subsequently, the coarse  $\kappa$  carbides grew into the adjacent grains with a  $\gamma/\kappa$  lamellar structure.

(2) The optimal combination of mechanical strength and ductility could be attained after aged at 625°C for 24 h. The specimen had good strength (UTS 1023MPa, YS 978MPa) with an excellent 44% elongation.

(3) After aged at 625°C for 96 h, the alloy still exhibited good 28% elongation; SEM investigations revealed that the fractured specimen had a typical ductile-type fracture behavior.

(4) Compared to the previous study concerning the mechanical properties of Fe-9%Al-30%Mn-2.0%C alloy, the microstructural effect of the  $\gamma/\kappa$  lamellar structure on the mechanical properties depended on its area fraction. Higher

area fraction of the  $\gamma/\kappa$  lamellar structure resulted in the embrittlement of the austenitic Fe-Al-Mn-C alloys.



## References

- [1] K. Sato, K. Tagawa, Y. Inoue, Scripta Metall. 22 (1988) 899.
- [2] K.H. Han, J.C. Yoon, W.K. Choo, Scripta Metall. 20 (1986) 33.
- [3] Y. Ikarashi, K. Sato, T. Yamazaki, Y. Inoue, M. Yamanaka: J. Mater. Sci. Letters 11 (1992) 733.
- [4] C.N. Hwang, T.F. Liu: Scripta Materialia 36 (1997) 853.
- [5] C.Y. Chao, L.K. Hwang, T.F. Liu: Scripta Metall. 29 (1993) 647.
- [6] K. Sato, K. Tagawa, Y. Inoue, Mater. Sci. Eng. A 111 (1989) 45.
- [7] W.K. Choo, J.H. Kim, J.C. Yoo, Acta Mater. 45 (1997) 4877.
- [8] C.Y. Chao, C.N. Hwang, T.F. Liu, Scripta Metall. 28 (1993) 109.
- [9] C.N. Hwang, C.Y. Chao, T.F. Liu, Scripta Metall. 28 (1993) 263.
- [10] K. Sato, K. Tagawa, Y. Inoue, Metall. Trans A 21 (1990) 5.
- [11] G.S. Krivonogov, M.F. Alekseyenko, G.G. Solov'yeva, Phys. Met. Metall. 39 (1975) 775.
- [12] I.S. Kalashnikov, O. Acselrad, A. Shalkevich, L.D. Chumakova, L.C. Pereira, J. Mater. Processing Technol. 136 (2003) 72.
- [13] K. Ishida, H. Ohtani, N. Satoh, R. Kainuma, T. Nishizawa, ISIJ Inter. 30 (1990) 680-686.
- [14] Y. Kimura, K. Handa, K. Hayashi, Y. Mishima, Intermetallics 12 (2004) 607-617.

- [15] Y. Kimura, K. Hayashi, K. Handa, Y. Mishima, Mater. Sci. Eng. A 329-331 (2002) 680.
- [16] C.S. Wang, C.G. Chao, T.F. Liu, "Mechanical Properties of an Fe-9Al-30Mn-2C Alloy", submitted to Materials Transactions (2007).
- [17] W.K. Choo, K.H. Han, Metall. Trans. A, 16 (1985) 5.
- [18] K.H. Han, W.K. Choo, Metall. Trans. A 14 (1983) 973.
- [19] K.H. Han, W.K. Choo, D.E. Laughlin, Scripta Metall. 22 (1988) 1873.
- [20] C.S. Wang, C.N. Hwang, C.G. Chao, T.F. Liu, "Phase Transitions in an Fe-9Al-30Mn-2.0C Alloy", accepted for publication in Scripta Mater. (2007).



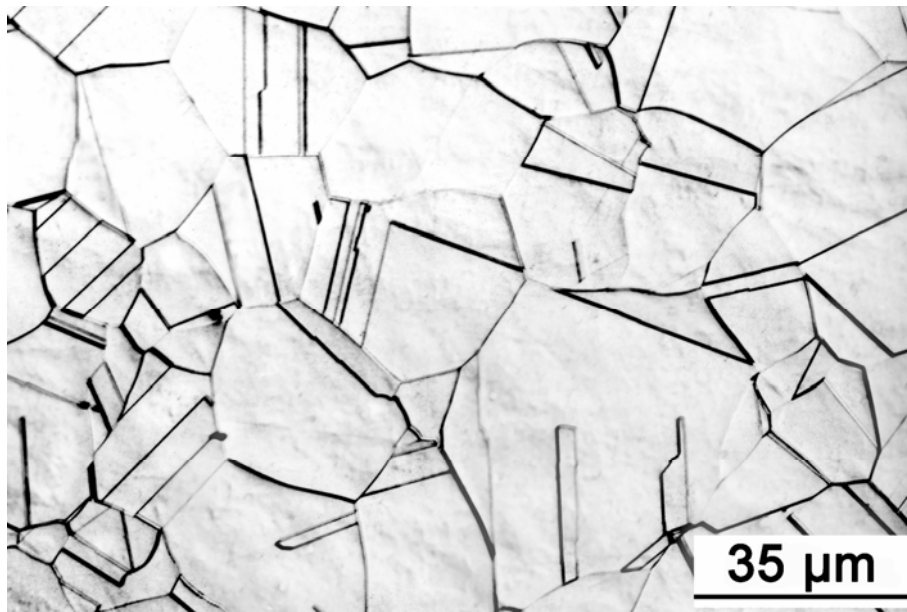
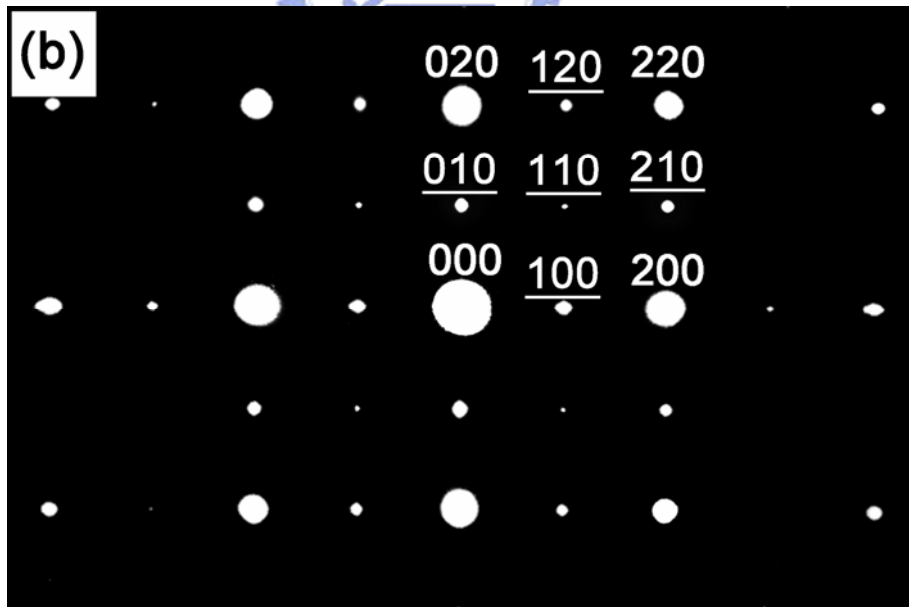
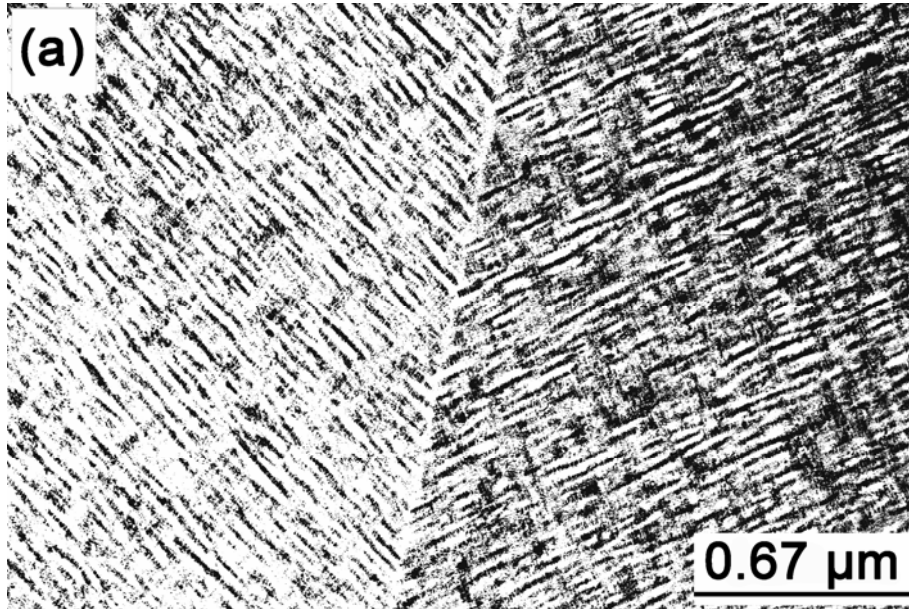


Figure 4.1 An optical micrograph of the as-quenched Fe-9%Al-30%Mn-1.0% C alloy.





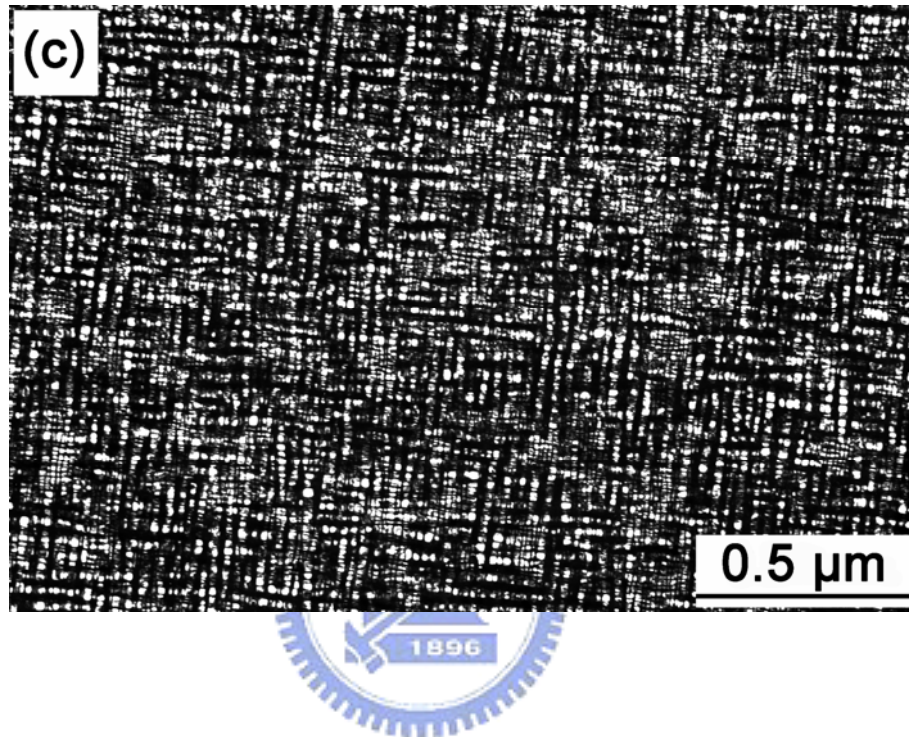


Figure 4.2 Transmission electron micrographs of the alloy aged at 625°C for 6 h. (a) bright-field, (b) a selected-area diffraction pattern taken from a mixed region of austenite matrix and fine  $\kappa'$  carbides. The foil normal is [001] ( $hkl$ : austenite matrix;  $\underline{hkl}$ :  $\kappa'$  carbide), and (c) dark-field electron micrograph taken with  $(100)_{\kappa'}$  superlattice reflection in the [001] zone.

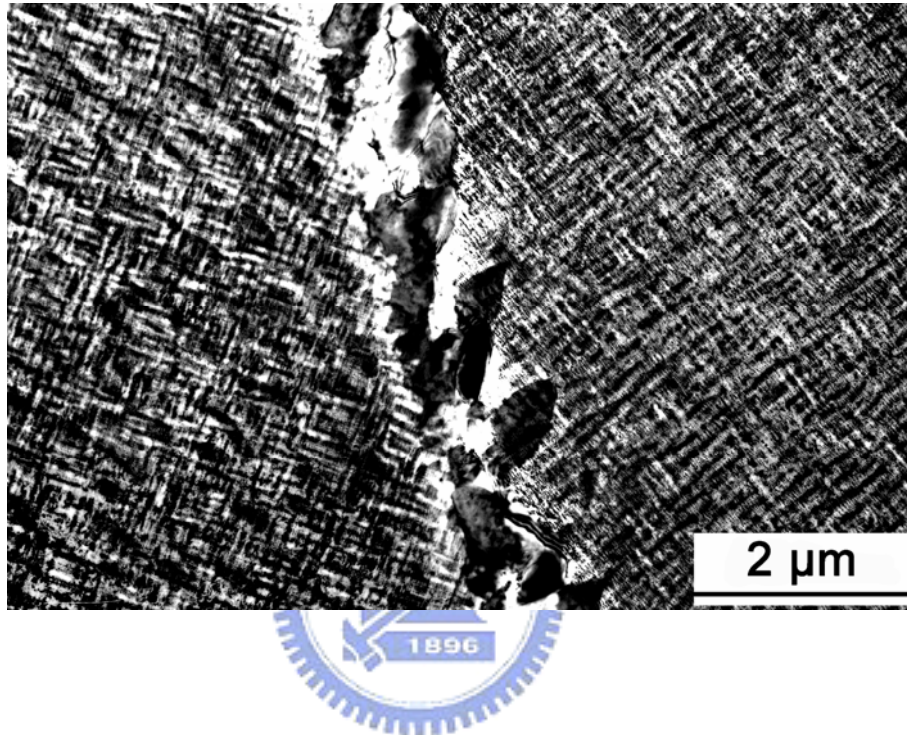
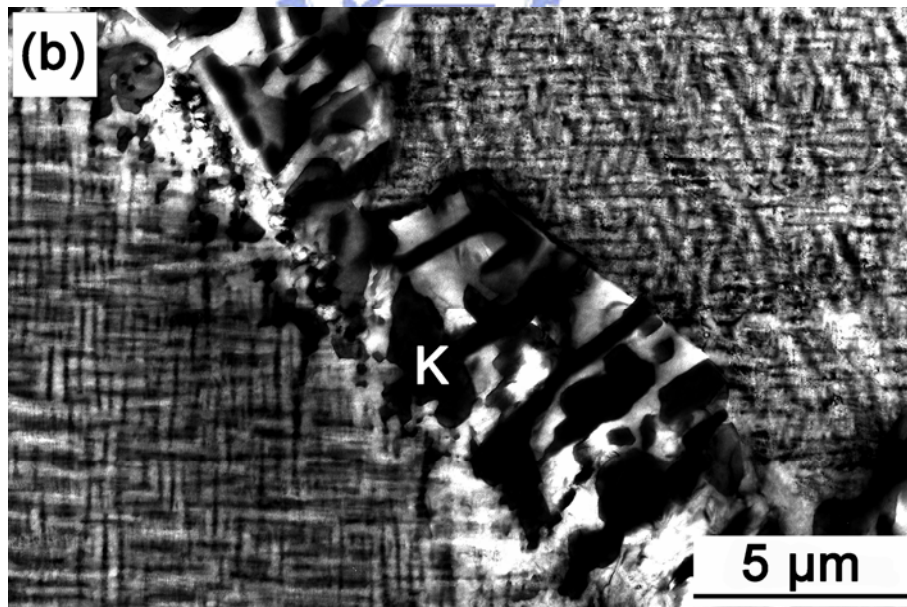
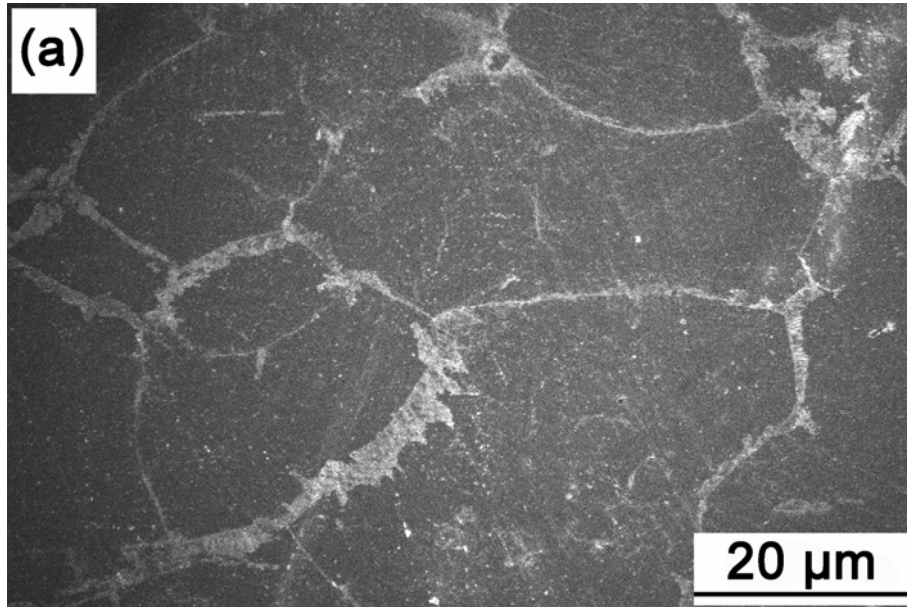


Figure 4.3 Bright-field electron micrograph of the alloy aged at 625°C for 24 h.



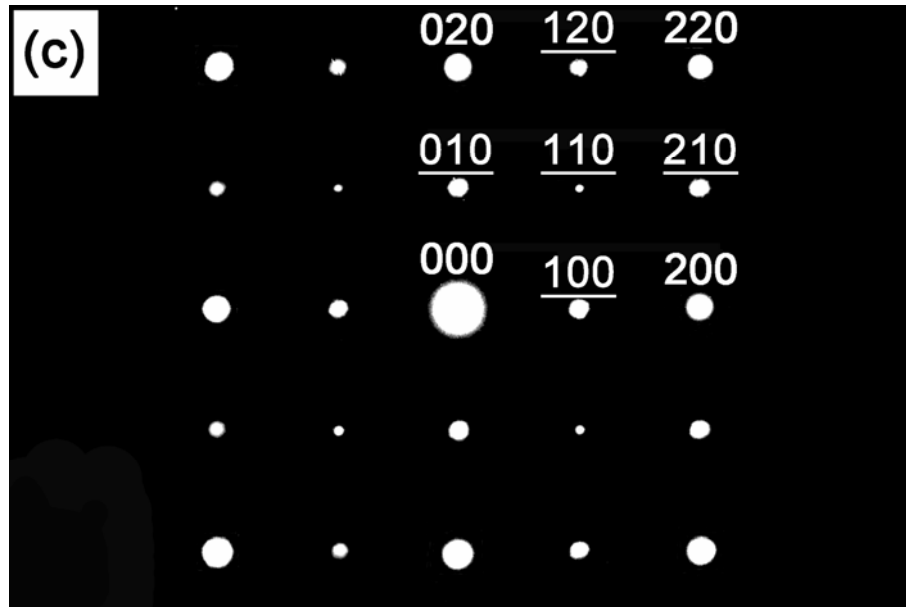


Figure 4.4 Micrographs of the alloy aged at 625°C for 96 h. (a) a SEM micrograph, (b)-(c) TEM micrographs: (b) bright-field, and (c) a selected-area diffraction pattern taken from an area covering the  $\kappa$  carbide marked as “K” and its surrounding austenite phase in (b). The foil normal is [001] ( $hkl$ : austenite phase;  $\underline{hkl}$ :  $\kappa$  carbide).

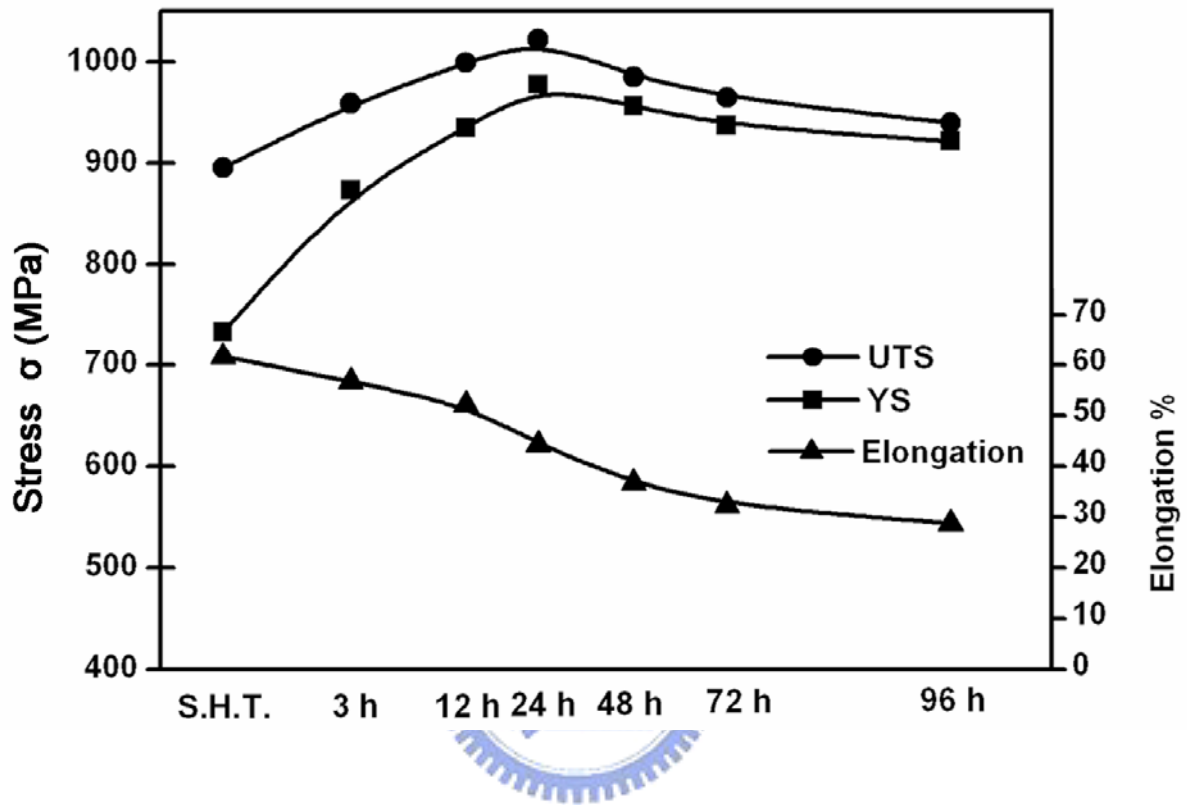


Figure 4.5 Tensile test results of the alloy in the as-quenched condition and after aged at 625°C for various times.

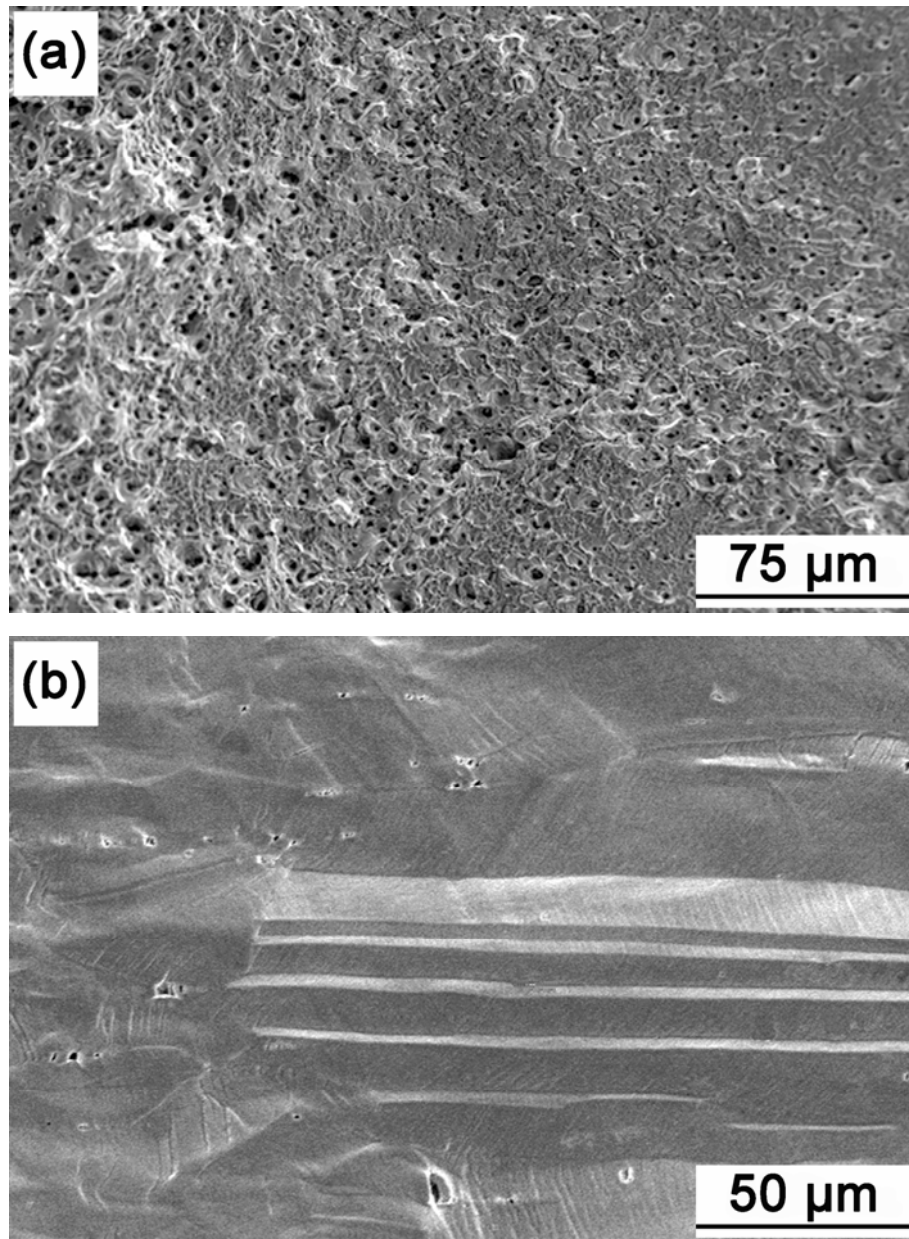


Figure 4.6 SEM micrographs of the fractured specimen aged at 625°C for 24 h. (a) fracture surface and (b) free surface contiguous to the fracture surface.

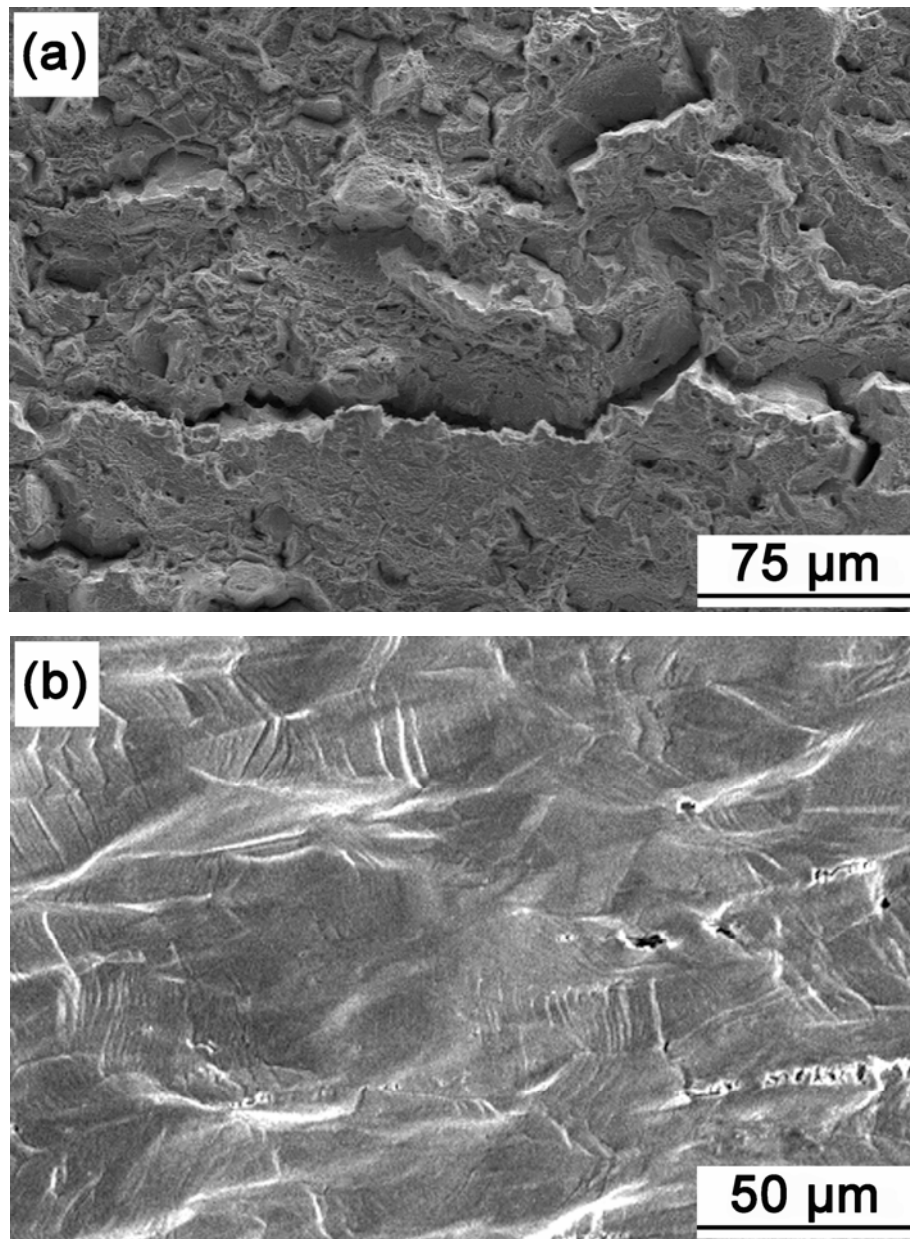


Figure 4.7 SEM micrographs of the fractured specimen aged at 625°C for 96 h. (a) fracture surface and (b) free surface contiguous to the fracture surface.



Table 4.1 Area fractions of the  $\gamma/\kappa$  lamellar structure.

Time	3 h	24 h	48 h	72 h	96h	
Area fraction	—	1.7	4.4	6.9	8.5	(1.0)C
(%)	19.3	45.7	—	—	100	(2.0)C



# Chapter 5.

## Summary



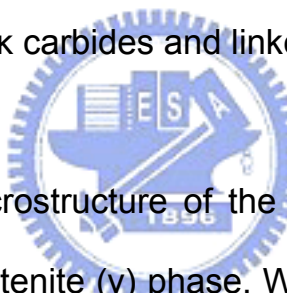
In the present study, phase transitions in an Fe-9Al-30Mn-2.0C alloy, mechanical properties of the Fe-9Al-30Mn-2.0C alloys, and mechanical properties of the Fe-9Al-30Mn-1.0C alloys have been examined. Based on the experimental results, some conclusions are given as follows:

[1]. In the as-quenched condition, the microstructure of the Fe-9wt.%Al-30wt.%Mn-2.0wt.%C alloy was austenite phase containing fine  $\kappa'$  carbides. The fine  $\kappa'$  carbides having an  $L'1_2$  structure were formed by spinodal decomposition during quenching. When the as-quenched alloy was aged at 550-900°C for moderate times, the fine  $\kappa'$  carbides grew within the  $\gamma$  matrix and coarse  $\kappa$  carbides started to occur on the  $\gamma/\gamma$  grain boundaries. When the alloy was aged at 900-1100°C, both of large and extremely fine  $\kappa$  and  $\kappa'$  carbides could be observed simultaneously within the austenite matrix. This feature has never been observed by other workers in the Fe-Al-Mn-C alloy systems before.

[2]. In the Fe-9wt.%Al-30wt.%Mn-2.0wt.%C alloy, the Al and Mn concentrations in the coarse  $\kappa$  carbides formed on the grain boundaries were found to vary drastically with the aging temperature.

[3]. The mechanical properties of the conventionally prepared austenitic Fe-9wt.%Al-30wt.%Mn-2.0wt.%C alloy were examined. Tensile tests revealed that the optimal combination of mechanical strength and ductility

of the alloy was the as-quenched specimen which had good ultimate tensile strength (UTS) of 1060 MPa with an excellent 57% elongation. When the as-quenched alloy was aged at 750°C for 3-96 h, both the tensile strength and ductility were significantly decreased. Interestingly, both of the mechanical strength and ductility of the as-quenched specimen were much better than those of the aged specimens. It is worthwhile to note that the mechanical properties of the austenitic Fe-Al-Mn-C alloys with C > 1.3 wt.% in the as-quenched condition have never been investigated by other workers before. In addition, the  $\gamma/\kappa$  lamellar structure of the aged specimens could not improve the tensile ductility because sub-cracks initiated at coarsened  $\kappa$  carbides and linked up to trigger cleavage.

- 
- [4]. The as-quenched microstructure of the Fe-9wt.%Al-30wt.%Mn-1.0wt.%C alloy was a single austenite ( $\gamma$ ) phase. When the alloy was aged at 625°C for short times, fine  $\kappa'$  carbides were observed to precipitate within the  $\gamma$  matrix. After prolonged aging at 625°C, the fine  $\kappa'$  carbides grew within the  $\gamma$  matrix and a  $\gamma + \kappa' \rightarrow \gamma + \kappa$  carbide reaction occurred on the grain boundaries. The mixture of ( $\gamma + \kappa$ ) had a lamellar structure. Tensile tests revealed that although the  $\gamma/\kappa$  lamellar structure occurred on the  $\gamma/\gamma$  grain boundaries after aged at 625°C for 96 h, the present alloy still exhibited good 28% elongation.

## List of Publications

### ● Journal Papers

1. C.S. Wang, C.N. Hwang, C.G. Chao and T.F. Liu, "Phase Transitions in an Fe-9Al-30Mn-2.0C Alloy", accepted for publication in Scripta Mater. (2007)
2. C.S. Wang, C.Y. Tsai, C.G. Chao and T.F. Liu, "Effect of Chromium Content on Corrosion Behaviors of Fe-9Al-30Mn-(3,5,6.5,8)Cr-1C Alloys", accepted for publication in Materials Transactions (2007)
3. C.S. Wang, C. Y. Tsai, C.G. Chao and T.F. Liu, "Corrosion behaviors of austenitic Fe-30Mn-7Al-xCr-1C alloys in 5% NaCl solution", submitted to Materials Characterization (2007)
4. C.S. Wang, C.G. Chao and T.F. Liu, "Mechanical Properties of an Fe-9Al-30Mn-2C Alloy", submitted to Materials Transactions (2007)
5. C.W. Su, C.S. Wang, J.W. Lee, C.G. Chao and T.F. Liu, "The effect of hot-dipped aluminum coatings on Fe-8Al-30Mn-0.8C alloy" submitted and revised to Surface and Coatings Technology (2007)

### ● Conference Papers

1. 王承舜, 曾傑享, 李堅璋, 蘇俊璋, 林志龍, 陳信良, 劉增豐 "鐵-9 鋁-30 錳-1.6 碳合金顯微結構與機械性質". (2006, 榮獲中國材料科學學會材料科學學生論文獎優等獎)

2. J.W. Lee, Y.H. Tuan, C.S. Wang and T.F. Liu, "Phase Transformations in Fe-9.02Al-30.0Mn-4.0Cr Alloy", Proceedings of The 2002 Annual Conference of The Chinese Society for Materials Science, A-4 (2002)
3. J.W.Lee, C.S.Wang, Y.H.Tuan, J.S.Lin and T.F.Liu, "Phase Transformations in an Fe-7.5Al-7Ni-1.4C Alloy", Proceedings of The 2001 Annual Conference of The Chinese Society for Materials Science, A-26 (2001)
4. C.H. Chen, J. Tan, C.P. Wang, C.S. Wang, S.Y. Yang, and T.F. Liu, "Phase Transformations in a Cu-14.2Al-10.0Ni Alloy", Proceedings of The 2000 Annual Conference of The Chinese Society for Materials Science, B-11 (2000)
5. C.S. Wang, I.S. Lo, C.P. Wang, C.H. Chen, S.Y. Yang, and T.F. Liu, "Phase Transformations in an Fe-8.8Al-30Mn-6Cr-1C Alloy", Proceedings of The 2000 Annual Conference of The Chinese Society for Materials Science, A-27 (2000)
6. C.P. Wang, Q.W. Yang, C.S. Wang, C.H. Chen, S.Y. Yang, J.W. Lee, and T.F. Liu, "Phase Transformations in an Fe-8Al-12Ni-2C Alloy", Proceedings of The 2000 Annual Conference of The Chinese Society for Materials Science, A-26 (2000)
7. S.Y. Yang, C.P. Wang, C.H. Chen, C.S. Wang, J.W. Lee, and T.F. Liu,

"Phase Transformations in an Fe-8.8Al-30.0Mn-6.0Mo-1.1C Alloy",  
Proceedings of The 2000 Annual Conference of The Chinese Society for  
Materials Science, A-25 (2000)

8. J.W. Lee, T.N. Lin, C.S.Wang and T.F. Liu, "Phase Transformations in an  
Cu-24.8Mn-30.0Al Alloy", Proceedings of The 1998 Annual Conference of  
The Chinese Society for Materials Science pp. 67-70 (1998)

